Ribosomal protein control of hematopoietic stem cell transformation through direct, non-canonical regulation of metabolism.

Bryan Harris[1,10], Dinesh K. Singh[1,10], Monika Verma[1], Shawn P. Fahl[1], Michele Rhodes[1], Shanna R. Sprinkle[2], Minshi Wang[1], Yong Zhang[1], Jaqueline Perrigoue[1], Rachel Kessel[3], Suraj Peri[4], Joshua West[5], Orsi Giricz[3], Jacqueline Boultwood[6], Andrea Pellagatti[6], KH Ramesh[3], Cristina Montagna[3], Kith Pradhan[3], Jeffrey W. Tyner[7], Brian K. Kennedy[8], Michael Holinstat[5], Ulrich Steidl[3], Stephen Sykes[9,10], Amit Verma[3,10], David L. Wiest[1,10,11]

1 – Nuclear Dynamics and Cancer Program, Fox Chase Cancer Center, Philadelphia, PA

2 – Department of Surgery, Duke University Medical Center, Durham, NC and Department of Biostatistics, University of North Carolina, Chapel Hill

3 – Department of Oncology, Albert Einstein College of Medicine, Montefiore Medical Center, Bronx, NY

4 – Biostatistics and Bioinformatics Facility, Fox Chase Cancer Center, Philadelphia, PA

5 – Department of Pharmacology, University of Michigan, Ann Arbor, MI, USA; Department of Internal Medicine, Division of Cardiovascular Medicine, University of Michigan, Ann Arbor, MI

6 – LLR Molecular Haematology Unit, NDCLS, John Radcliffe Hospital, and NIHR Biomedical Research Centre, Oxford, United Kingdom

7 – Division of Hematology and Medical Oncology, Oregon Health & Science University Knight Cancer Institute, Portland, OR

8 – Departments of Biochemistry and Physiology, Yong Loo Lin School of Medicine, National University of Singapore, Singapore

9 – Department of Pediatrics, Washington University School of Medicine, St. Louis, MO

10 – Contributed equally

11 – Lead contact: David L. Wiest, Fox Chase Cancer Center, Nuclear Dynamics and Cancer Program, R364, 333 Cottman Avenue, Philadelphia, PA 19111; Tel – 215-728-2966; Fax – 215-728-2412; Email – david.wiest@fccc.edu

Summary: We report here that expression of the ribosomal protein, RPL22, is frequently reduced in human myelodysplastic syndrome (MDS) and acute myelogenous leukemia (AML); reduced RPL22 expression is associated with worse outcomes. Mice null for Rpl22 display characteristics of an MDS-like syndrome and develop leukemia at an accelerated rate. Rpl22-deficient mice also display enhanced hematopoietic stem cell (HSC) self-renewal and obstructed differentiation potential, which arises not from reduced protein synthesis but from increased expression of the Rpl22 target, ALOX12, an upstream regulator of fatty acid oxidation (FAO). The increased FAO mediated by Rpl22-deficiency also persists in leukemia cells and promotes their survival. Altogether, these findings reveal that Rpl22 insufficiency enhances the leukemia potential of HSC via non-canonical de-repression of its target, ALOX12, which enhances FAO, a process that may serve as a therapeutic vulnerability of Rpl22 low MDS and AML leukemia cells.

Keywords: ribosomal protein, Alox12, fatty acid oxidation, hematopoietic stem cell, MDS, AML, metabolism

Highlights:

- RPL22 insufficiency is observed in MDS/AML and is associated with reduced survival
- Rpl22-deficiency produces an MDS-like syndrome and facilitates leukemogenesis
- Rpl22-deficiency does not impair global protein synthesis by HSC
- Rpl22 controls leukemia cell survival by non-canonical regulation of lipid oxidation

eTOC: Rpl22 controls the function and transformation potential of hematopoietic stem cells through effects on ALOX12 expression, a regulator of fatty acid oxidation.

INTRODUCTION:

Ribosomopathies are a group of inherited diseases resulting from mutations or deletions of ribosomal protein (RP) encoding genes or factors that facilitate ribosome biogenesis (Danilova and Gazda, 2015; Kampen et al., 2020; Narla and Ebert). This class of diseases is characterized by defects in hematopoiesis that often culminate in complete bone marrow failure, with many patients progressing to the development of myelodysplastic syndromes (MDS) and acute myelogenous leukemia (AML) (Nakhoul et al., 2014), as a result of the aberrant function of hematopoietic stem cells (HSC) (Corey et al., 2007). The association between the inactivation of RP and increased risk for myeloid malignancy has been known for some time, but the mechanistic link remains unclear and controversial (De Keersmaecker et al., 2015; (Sulima et al., 2019). Some evidence suggests that RP mutations disrupt hematopoiesis and increase cancer risk by generalized impairment of ribosome function (De Keersmaecker et al., 2015; Khajuria et al., 2018; Norris et al., 2021), while others suggest that particular RNA-binding RP are capable of performing specific regulatory functions (Genuth and Barna, 2018a; Kang et al., 2021; Kondrashov et al., 2011). Indeed, recent evidence suggests that *RPS14* haploinsufficiency promotes the 5q- subtype of MDS through S100A8-mediated induction of p53 (Schneider et al., 2016); however, the mechanistic link for this effect remains to be established. Several other studies have highlighted “extraribosomal”, regulatory functions of RP involving their ability to bind to RNA targets and modulate processes, including pre-mRNA splicing and translation (Ivanov et al., 2006; Kang et al., 2021; Singh et al., 2009). These findings highlight a need to systematically investigate the contribution of RP inactivation, or reductions in their expression, to the etiology of myeloid neoplasms in order to gain insight into how the lost regulatory functions of RP might contribute to malignant hematopoiesis.

One RP of particular interest is Rpl22, an RNA-binding RP that binds to the 28S rRNA and is located on its exterior surface of the 60S ribosomal subunit (Auger-Buendia et al., 1979; Sanz

et al., 2009). While this highly conserved RP is ubiquitously expressed in mammalian tissues, it is distinguished from many other RP in that it is not required for ribosome biogenesis or global protein translation (O'Leary et al., 2013). Moreover, the germline ablation of the *Rpl22* gene in mice does not result in lethality or gross developmental abnormalities (Anderson et al., 2007). Rather, Rpl22-deficiency causes selective alterations in lymphopoiesis, consistent with the loss of a regulatory function on which selected cell types are particularly dependent. Indeed, Rpl22-deficiency attenuates the development of B lymphocytes and $\alpha\beta$ lineage T lymphocytes in a p53-dependent manner, while sparing other lineages, including $\gamma\delta$ T cells (Anderson et al., 2007; Fahl et al., 2015). Moreover, Rpl22 regulates the emergence of fetal HSC by controlling the translation of *Smad1* mRNA (Zhang et al., 2013). Finally, *RPL22* mutations and deletions have been observed in human T acute lymphoblastic leukemia (T-ALL), and Rpl22 loss promotes lymphoma development in a mouse model of T-ALL, suggesting that it functions as a tumor suppressor (Rao et al., 2012).

The ability of Rpl22 to regulate lymphoid development and transformation, as well as fetal HSC emergence, led us to investigate whether Rpl22 also plays a role in regulating the function of adult HSC and their potential for transformation into myeloid malignancy. Here we show that reduced expression of *RPL22* is seen in human MDS and AML; and, is linked to poor outcomes and that Rpl22 loss in mice predisposes to transformation, not though alterations in global protein synthesis, but rather through alterations in HSC metabolism.

RESULTS:

RPL22 expression is reduced in human MDS and AML

To assess the changes in RP expression levels in human myeloid neoplasms, we performed gene expression analysis of $CD34^+$ hematopoietic progenitor cells of 183 MDS patients. This analysis revealed that *RPL22* is one of the most significantly reduced RP in this disease (**Fig. 1A,B**). We also observed that reduced *RPL22* expression was associated with lower hemoglobin (Hb) levels, a marker of MDS severity (**Fig. 1C**)(Gerstung et al., 2015). Since MDS often progresses to AML, we evaluated *RPL22* expression in bulk tumor from AML patients using data obtained from the Beat AML consortium and TCGA(Tyner et al., 2018). Strikingly, *RPL22* expression was significantly decreased amongst most AML patients compared to healthy controls (**Fig. 1D)**. We further examined *RPL22* expression levels in the immature cells from which this disease originates, by stringently sorting hematopoietic stem and progenitor cell (HSPC) populations from patients diagnosed with AML (**Fig. 1E-G**)(Barreyro et al., 2012). From these analyses, we observed a significant reduction of *RPL22* mRNA in the leukemia initiating populations comprising long-term HSC (LT-HSC; $Lin^-CD34^+CD38^-CD90^+$), short-term HSC (ST-HSC; $Lin^-CD34^+CD38^-CD90^-$), and granulocyte-macrophage progenitors (GMP; $Lin^-CD34^+CD38^+CD123^+CD45RA^+$) of patients with higher risk AML (associated with complex karyotype; CK), compared to identically sorted cells from age-matched, healthy controls (**Fig. 1E-G**) (Grimwade and Hills, 2009; Lapidot et al., 1994). Moreover, reduced expression of *RPL22* was associated with more aggressive AML, since the patients with low *RPL22* expression (bottom quartile) from the TCGA AML cohort exhibited reduced overall survival (**Fig. 1H**). Using fluorescent *in situ* hybridization (FISH) analysis in another independent cohort of MDS/AML samples, we found that the *RPL22* locus was more frequently deleted in progenitor cells from both MDS and AML patients (**Fig. 1I**). Approximately 40% of MDS patients and 27% of AML patients showed evidence of increased *RPL22* deletion, with more of these patients being represented in the high-risk MDS and secondary AML groups

(Fig. 1J). Collectively, these data indicate that *RPL22* expression is frequently reduced in MDS/AML patients, including in their HSPC, and that low *RPL22* expression is associated with reduced survival, and thus more aggressive myeloid disease.

Rpl22-deficient mice display an MDS-like phenotype

To determine whether Rpl22 regulates MDS and AML progression, we assessed whether loss of *Rpl22* disrupted murine hematopoiesis. Similar to MDS patients, *Rpl22*$^{-/-}$ mice displayed a significant reduction in red blood cells (RBC) with increased mean corpuscular volume (MCV**)**, as is observed in macrocytic anemia seen in MDS (**Fig. 2A,B**) (Linman and Bagby, 1976). Rpl22-deficient mice also exhibited evidence of erythroid and myeloid dysplasia (**Fig. S1B,C)**, and an increased frequency of megakaryocytes (**Fig. 2C**). Finally, the bone marrow of Rpl22-deficient mice contained ~20% more CD34+ cells **(Fig. 2D)** and an expansion of granulocyte-macrophage progenitors (GMP; LK/CD34^{+}FCγR^{high}; **Fig. 2E**), as is typically observed in higher-risk MDS and AML patients (Will et al., 2012).

Since the alterations in hematopoiesis observed in MDS patients result from impaired function of their expanded HSC population, we sought to determine if these same abnormalities characterized the HSC in *Rpl22*$^{-/-}$ mice (Miraki-Moud et al., 2013; Woll et al., 2014). Indeed, both lineage-, Sca-1^{+}, c-Kit^{+}, (LSK) cells and HSC defined by SLAM markers (LSK/CD48^{-}CD150^{+}) were increased in the bone marrow of *Rpl22*$^{-/-}$ mice, relative to wild-type littermate controls (**Fig. 2F,G; Fig. S2A,B**) (Kiel et al., 2005),(Oguro et al., 2013). This expansion was associated with an increased number of proliferating cells, as HSC and other progenitor populations in *Rpl22*$^{-/-}$ mice exhibited greater BrdU incorporation (**Fig. 2H**). *Rpl22-/-* HSC also exhibited a modest increase in Ki-67 staining, compared to *Rpl22*$^{+/+}$ controls (**Fig. S2C;** p=0.06).

Because inactivation of other RP (e.g., *RPS14)* has been reported to impair hematopoiesis by activation of p53 we employed p53-deficient mice to determine if the expansion of pre-malignant HSC in *Rpl22*$^{-/-}$ mice was p53-dependent (Deisenroth and Zhang, 2010; Schneider et al.). Interestingly, we found that p53-deficiency failed to suppress the expansion of LSK and HSC observed in Rpl22-deficient mice (**Fig. S2D,E**). Thus, as occurs in MDS patients, Rpl22-deficient mice display an expansion of HSC in the marrow; however, this expansion is not dependent upon p53, as it is not corrected by p53-deficiency. We previously reported that Rpl22 and its paralog Rpl22-Like1 (Rpl22l1 or Like1) antagonistically control the emergence of embryonic HSC, with Rpl22 repressing emergence and Like1 inhibiting that repression (Zhang et al., 2013). The expansion of adult HSPC in Rpl22-deficient mice is also dependent upon Like1, since ablation of one allele of *Rpl22l1* was sufficient to markedly reduce the number of both LSK and HSC in adult bone marrow **(Fig. S2F-H)**(Kuhn et al., 1995; Zhang et al., 2017).

Rpl22 loss impairs HSC function

The alterations in hematopoiesis observed in MDS patients have previously been shown to result from dysfunctional HSC (Elias et al., 2014; Miraki-Moud et al., 2013; Woll et al., 2014). To determine if this was also true of the altered hematopoiesis observed in Rpl22-deficient mice, we performed competitive bone marrow transplantation assays using allotype-marked (CD45.2) *Rpl22*$^{-/-}$ or *Rpl22*$^{+/+}$ HSC combined with whole bone marrow competitor (WBM, CD45.1). Analysis of peripheral blood 20 weeks after transplantation revealed that *Rpl22*$^{-/-}$ HSC were significantly less capable of reconstituting hematopoiesis than *Rpl22*$^{+/+}$ HSC, as *Rpl22*$^{-/-}$ HSC produced very few peripheral blood leukocytes (**Fig. 3A**). Moreover, the few leukocytes that were produced by Rpl22-deficient HSC were profoundly biased toward the myeloid fate (CD11b^{+}Gr-1^{+}; **Fig. 3B**), consistent with the basal myeloid-bias observed in the donor *Rpl22*$^{-/-}$ mice and in MDS patients (Saultz and Garzon, 2016).

The failure of *Rpl22*$^{-/-}$ HSCs to reconstitute hematopoiesis could have resulted from their failure to engraft, or, alternatively, from failure to produce mature hematopoietic cell lineages following engraftment. To evaluate the extent of engraftment by Rpl22-deficient HSC, we assessed donor chimerism in the bone marrow of transplanted mice. While *Rpl22*$^{-/-}$ HSC contributed less to overall bone marrow cellularity than did *Rpl22*$^{+/+}$ HSC (**Fig. 3C**), the contribution of *Rpl22*$^{-/-}$ HSC to the recipient bone marrow was nearly 2-times (1.8 fold) greater than to peripheral blood (**Fig. S3**). Together these data suggest that the MDS-like phenotype observed in *Rpl22*$^{-/-}$ mice results from HSC dysfunction, where Rpl22-deficient HSC are capable of self-renewal, as evidenced by their ability to engraft and expand in the bone marrow, but are impaired in their ability to produce lineage-committed downstream progenitors or peripheral leukocytes.

To identify the stages of hematopoiesis impaired by Rpl22-deficiency, we assessed the contribution of *Rpl22*$^{-/-}$ HSC to particular hematopoietic progenitor populations, relative to that of *Rpl22*$^{+/+}$ HSC. Interestingly, transplanted *Rpl22*$^{-/-}$ HSCs produced LSK, HSC, and multipotent progenitors (MPP, LSK/CD150^{-}CD48^{-}) as effectively as *Rpl22*$^{+/+}$ HSCs (**Figs. 3D,E and S3B**). However, development of *Rpl22*$^{-/-}$ progenitors beyond the MPP stage was more severely impaired, as LK cells, and all of their subsets (GMP; LK/CD34^{-}FCγR^{low} megakaryocyte-erythroid progenitors or MEP; and LK/CD34^{+}FCγR^{low} common myeloid progenitors or CMP), were reduced relative to mice transplanted with *Rpl22*$^{+/+}$ HSC, with GMP and MEP exhibiting the most profound reductions (**Fig. 3F,G**). Consequently, Rpl22-deficient HSC are capable of engraftment, expansion, and generation of MPP, but are impaired in their ability to give rise to downstream, committed progenitors.

Rpl22-deficiency alters the metabolism of HSC

To determine how Rpl22-deficiency impairs HSC function, we performed whole transcriptome analysis on HSC from *Rpl22*$^{+/+}$ and *Rpl22*$^{-/-}$ mice. From this analysis, we found that Rpl22-deficiency altered the expression of nearly 600 genes (**Fig. S4** and **Table S1**). Gene ontology (GO) analysis using the Cellular Components Database revealed that Rpl22-deficiency most significantly affects the expression of clusters of genes associated with the ribosome and mitochondria (**Fig. 4A and Table S2).** Because HSC function has been reported to be impaired by reductions in protein synthesis, and because ribosomal protein mutations are linked to significant decreases in global protein synthesis, we sought to determine if Rpl22-deficiency was impairing HSC function by attenuating protein synthesis (Khajuria et al., 2018; Liu et al., 2012; Signer et al., 2014). To test this possibility, we measured protein synthesis in HSC *in situ*, by monitoring O-propargyl-puromycin (OPP) incorporation into nascent polypeptides using flow cytometry (Liu et al., 2012; Signer et al., 2014). Surprisingly, we observed that the incorporation of OPP into newly synthesized proteins by *Rpl22*$^{-/-}$ HSC (red) was equivalent to that incorporated by *Rpl22*$^{+/+}$ HSC (blue) (**Fig. 4B**). Therefore, in contrast to what has been observed for HSC upon inactivation of other RP, this analysis revealed the unexpected finding that the alteration of HSC function caused by Rpl22-deficiency is not associated with an attenuation of global protein synthesis (Khajuria et al., 2018; Schneider et al., 2016; Signer et al., 2014; Teng et al., 2013).

Global protein synthesis was not impaired by Rpl22 loss. Consequently, we sought to determine if altered mitochondrial function was contributing to the impaired function of Rpl22-deficient HSC, since mitochondrial function, particularly oxidative phosphorylation and fatty acid oxidation (FAO), was another GO class exhibiting an altered expression signature in Rpl22-deficient HSC (**Fig. 4A,C**; **Table S2**). To determine if these changes in gene expression altered mitochondrial function, we performed metabolic analysis on *Rpl22*$^{+/+}$ and *Rpl22*$^{-/-}$ LSK cells. We observed no differences in mitochondrial biomass or in extracellular acidification rate (ECAR), a surrogate measure of glycolysis (**Fig. S5A,B**). Consistent with the lack of change in ECAR,

pAMPK, ATP, and lactate levels were also unaffected by Rpl22-deficiency **(Fig. S5C)**. *Rpl22*$^{-/-}$ LSK did exhibit reduced oxygen consumption, suggesting a reduction in cellular capacity to mediate oxidative respiration (**Fig. S5D**). The reduction in oxygen consumption is associated with reduced expression of a key component of the electron transport chain, *Atp5e*, which is required for oxygen consumption by electron transport complex (ETC) IV (**Table S1)**(Mayr et al., 2010). Interestingly, the expression of a number of genes involved in fatty acid metabolism was increased in Rpl22-deficient HSC (**Fig. 4C**). These alterations in gene expression are noteworthy because increased dependence on fatty acid oxidation (FAO) has been implicated in both HSC self-renewal, leukemic stem cell function, and cancer stem cell function (Ito et al., 2012; Stevens et al., 2020; Vacanti et al., 2014). Consistent with the increased expression of genes involved in lipid oxidation, FAO was increased in *Rpl22*$^{-/-}$ LSK (**Fig. 4D**). It should be noted that attenuating FAO using the FAO inhibitor, Etomoxir (Antinozzi et al., 1998; Tutwiler et al., 1985), did not restore oxygen consumption in *Rpl22-/-* HSPC, suggesting that the reduction of oxygen consumption and the increased FAO exhibited by Rpl22-deficient LSK are not mechanistically interdependent.

Since increased FAO has been implicated in the self-renewal of HSC, we asked if explanted Rpl22$^{-/-}$ HSCs exhibited a prolonged retention of their SLAM-marked HSC phenotype (LSK, CD150^{+}, CD48^{-}) upon culture *in vitro* (Ito et al., 2012). Indeed, whereas a significant proportion of *Rpl22*$^{+/+}$ HSC lost their HSC phenotype after two days in culture, it was fully retained by *Rpl22*$^{-/-}$ HSC **(Fig 5A)**. Moreover, retention of the HSC phenotype by *Rpl22*$^{-/-}$ HSC was dependent on FAO, as it was abrogated by inhibition of FAO using Etomoxir (**Fig 5B)** (Antinozzi et al., 1998; Tutwiler et al., 1985). Blockade of FAO was not cytotoxic to *Rpl22*$^{-/-}$ HSC, but instead induced their differentiation into MPP **(Fig 5B)**. *Rpl22*$^{-/-}$ HSPC also exhibited enhanced function, as they retained a greater capacity to form colonies in methylcellulose following serial passage. This capability was also attenuated by pharmacologic inhibition of FAO (**Figs. 5C and S5E**). Together these findings suggest that the increased self-renewal and inability of *Rpl22*$^{-/-}$ HSC to

support the development of downstream committed progeny results from an alteration in cellular metabolism. Specifically, *Rpl22*$^{-/-}$ HSC exhibit both a reduced ability to perform oxidative phosphorylation, a generator of the physiologic oxygen radicals required to promote differentiation, and enhanced FAO, which promotes self-renewal (Ito et al., 2012; Lyublinskaya et al., 2015).

Rpl22 regulates the expression of Alox12

Because Rpl22 is an RNA binding protein, we hypothesized that Rpl22 might control FAO in HSC by modulating the activity of mRNA targets encoding regulators of this process. Using M-fold to predict RNA secondary structure, we found that several of the transcripts encoding regulators of FAO bear the consensus stem-loop structure recognized by Rpl22 (**Fig. S6A-E)**. Amongst these differentially expressed targets **(Fig. 4C)**, arachidonate lipoxygenase-12 (Alox12) was of particular interest, both because there were two consensus Rpl22 binding sites in the coding regions of both mouse *Alox12* and human *ALOX12* (**Fig. S6B,F),** and because Alox12 converts polyunsaturated fatty acids to the activating ligands for a master transcriptional regulator of FAO, PPARδ (Almeida et al., 2009; Kuhn et al., 2015). Accordingly, we wished to determine whether the increase in Alox12 played an important role in the dysregulation of HSPC function by Rpl22-loss and how Rpl22 regulated its expression. Analysis of Alox12 protein and mRNA levels revealed that the increase in Alox12 protein levels exceeded that of its mRNA **(Fig. 5D)**, suggesting post-transcriptional regulation. The increase in Alox12 expression was accompanied by increased generation of the arachidonic acid breakdown product it generates, 12S-HETE **(Fig. 5E).** To determine whether the induction of Alox12 expression plays an important role in altering the behavior of *Rpl22*$^{-/-}$ HSPC, we crossed the *Rpl22-/-* mice to mice bearing genetically ablated *Alox12* alleles and assessed the effect on colony formation by LSK (**Figs. 5F**)(Sun and Funk, 1996). Genetic ablation of *Alox12* attenuated colony formation by Rpl22-deficient LSK **(Fig. 5G)**. Conversely, overexpression of Alox12 increased the ability of *Rpl22+/+* LSK to form colonies **(Fig.**

5H), indicating that the increase in Alox12 expression in Rpl22-deficient LSK was both necessary and sufficient to support their increased colony forming capacity.

Having determined that Alox12 plays an important role in regulating HSPC function, we next wished to determine how its expression was controlled by Rpl22. To determine if Rpl22 bound to the two consensus binding sites in the coding sequence of *Alox12* mRNA, we performed electrophoretic-mobility shift analysis (EMSA) **(Fig. 5H).** EMSA analysis confirmed that Rpl22 bound strongly to positive control RNA, EBER1, but not negative control EBER2 (Dobbelstein and Shenk, 1995). Moreover, Rpl22 also bound to the second predicted binding site (BS2) of *Alox12*, but not to the first predicted binding site (BS1) or to NBS, an RNA sequence between BS1 and BS2 that lacks the Rpl22 target motif (**Fig. 5H**). In addition to its ability to bind to *Alox12* mRNA, Rpl22 is capable of post-transcriptionally repressing the expression of Alox12 upon ectopic expression in Rpl22-deficient mouse embryonic fibrobasts (MEF) **(Fig. 5I).** Rpl22 appears to be regulating Alox12 by controlling its inclusion in actively translating polysomes, since Rpl22 reintroduction into Rpl22-deficient MEF displaces *Alox12* mRNA for heavy polysomes **(Fig. 5J).** Finally, when the Rpl22 binding site in *Alox12* mRNA (BS2) is appended to a heterologous mRNA (GFP), it confers responsiveness to Rpl22 regulation **(Fig. 5K)**. Collectively, these results support a model where Rpl22 controls FAO and HSC function by directly binding *Alox12* mRNA and regulating protein expression.

Rpl22-deficiency promotes the development of leukemia

Since enhanced self-renewal and impaired differentiation characterize a premalignant state, we reasoned that *Rpl22*$^{-/-}$ HSC should be predisposed to leukemic transformation (Warner et al., 2004). Consistent with this perspective, comparison of the expression signature of *Rpl22*$^{-/-}$ HSC to the OMIM Disease database revealed an association with leukemia, particularly genes

regulated by the MLL-AF9 oncogenic fusion (**Figs. 6A and S7A**). Consequently, we assessed whether *Rpl22*$^{-/-}$ HSC were predisposed to transformation using the MLL-AF9 oncogene knock in model of AML (Corral et al., 1996; Horton et al., 2013). Indeed, *Rpl22*$^{-/-}$ MLL-AF9 knock in mice exhibited a far greater leukemic burden at 15 weeks of age, as evidenced by splenic weight (**Figs. 6B and S7B,C**). Furthermore, Rpl22-deficient MLL-AF9 knock in mice developed and succumbed to leukemia much more rapidly than their *Rpl22*$^{+/+}$ counterparts (**Fig. 6C**).

Rpl22-deficient leukemias are dependent on ALOX12

Since increased FAO was required for the enhanced self-renewal exhibited by *Rpl22*$^{-/-}$ HSC, we next asked if enhanced FAO also contributed to increased leukemic potential of the Rpl22-deficient MLL-AF9 leukemia cells. We found that, similar to non-transformed HSCs, MLL-AF9 transformed LSK from *Rpl22*$^{-/-}$ mice exhibited increased FAO (**Fig. 7A**); The *Rpl22-/-* leukemia did not exhibit the reduction in oxygen consumption observed in primary Rpl22-deficient LSK, suggesting that this defect is not retained during transformation **(Fig. S7D).** The increase in FAO appears to play an important role in maintaining the leukemic potential of *Rpl22-/-* leukemia cells, since treatment with the FAO inhibitor, Etomoxir, was far more effective in inhibiting colony formation by *Rpl22*$^{-/-}$ leukemia cells than by their *Rpl22*$^{+/+}$ counterparts (**Fig. 7B**). Moreover, pharmacologic inhibition of Alox12 activity, using the drug baicalein, preferentially attenuated colony formation by Rpl22-deficient leukemia cells (**Fig. 7C**). To gain insight into how Alox12 activity was promoting leukemic colony formation by regulation of FAO, we explored the role of PPARδ, a master regulator of FAO that is activated by the lipid ligands generated by Alox12 (Ito et al., 2012). Indeed, shRNA knockown of *Ppard* selectively attenuated colony formation by *Rpl22-/-* leukemias, indicating that Rpl22 loss promotes colony formation by upregulation of Alox12, which activates FAO by generating the ligands that activate the master regulator of FAO, PPARδ.

To assess whether the importance of Alox12 was restricted to *in vitro* colony formation, or alternatively, is also important to leukemic progression *in vivo*, we isolated *Rpl22+/+* and *Rpl22-/-* leukemias that arose in the MLL-AF9 knock in mice **(Fig. 7E)**. Alox12 expression was markedly elevated in the *Rpl22-/-* leukemia **(Fig. 7E).** To determine if Alox12 plays a critical role in the pathogenesis of leukemia development, we identified shRNA that knocked down Alox12 expression **(Fig. S7E)**, and then assessed the effect on leukemia pathogenesis in vivo by zebrafish transplantation **(Figs. 7F and S7F)**. Zebrafish embryos were injected with leukemias at 2 days post fertilization (dpf) and their survival was monitored for an additional 6days. Importantly, the *Rpl22-/-* leukemias more aggressively supported leukemia pathogenesis, and this was completely reversed by Alox12 knockdown *(***Figs. 7F and S7F).** Alox12 knockdown had not appreciable effect on the capacity of the *Rpl22+/+* leukemias to promote disease. Taken together, these data indicate that the capacity of Rpl22 loss to enhance leukemic progression in vivo is dependent upon the induction of Alox12.

DISCUSSION:

In this report, we provide evidence that RP-insufficiency alters HSC function and increases the predisposition to leukemia through a novel mechanism that does not involve attenuation of global protein synthesis. Instead, HSC function is altered because of the dysregulated expression of selected Rpl22 gene targets that impact metabolism. *RPL22* expression is reduced in human MDS and AML, including at the stem cell level, and is associated with reduced survival. The link between reduced *RPL22* expression and poor survival is also observed in a mouse leukemia model lacking Rpl22. As indicated, the mechanistic link between Rpl22 loss and enhanced leukemogenic potential is distinct from that of other cases of RP insufficiency in that it does not involve attenuation of global protein synthesis (Khajuria et al., 2018; Schneider et al., 2016; Signer et al., 2014). Instead, *Rpl22* inactivation creates a premalignant state characterized by enhanced HSC self-renewal and impaired generation of downstream committed progenitors, by altering metabolism. Specifically, Rpl22-loss decreases oxygen consumption and increases the dependence of HSC and leukemias on FAO. These observations are consistent with previous reports demonstrating that enhanced FAO promotes HSC self-renewal, leukemic stem cell function, and cancer stem cell activity, including leukemia stem cells (Ito et al., 2012; Schell et al., 2014; Stevens et al., 2020; Tabe et al., 2020; Vacanti et al., 2014). Importantly, we also establish a novel molecular link between Rpl22-insufficiency and enhanced FAO that is mediated by a regulator of FAO, Alox12, whose expression is controlled post-transcriptionally through Rpl22 binding to its mRNA. Together, these observations indicate that Rpl22 controls HSC function and transformation potential through effects on its target, Alox12, which regulates of FAO.

We have previously reported that Rpl22 is not essential for life, but does act to regulate normal development and transformation through a variety of mechanisms that differ depending on the stage of development or cell type involved. Indeed, we had previously reported that the antagonistic balance between Rpl22 and its highly homologous paralog, Rpl22-Like1 (Rpl22l1 or

Like1), controls the emergence of embryonic HSC by controlling the translation of *Smad1* mRNA (Zhang et al., 2013). Rpl22 regulation of the behavior of adult stem cells is also dependent upon Like1, since Like1-insufficiency attenuates the HSC expansion observed in Rpl22-deficient mice, though this presumably does not involve effects on Smad1 expression, since Smad1 is dispensable in adult HSC (Singbrant et al., 2010). Rpl22 also regulates the development of B and T lymphocytes beyond their pre-receptor checkpoint stages (Fahl et al., 2015; Solanki et al., 2016). At least in T cells, the regulation of this transition is mediated through control of the unfolded protein response (UPR) or endoplasmic reticulum (ER) stress signaling (Solanki et al., 2016). The relatively lineage restricted requirement for Rpl22 to regulate ER stress signaling appears to be limited to cells experiencing unusually abrupt transitions from quiescence to rapid proliferation, as is observed at the pre-receptor checkpoints (Taghon et al., 2006). This does not appear to be relevant in cells that undergo less abrupt proliferative transitions, such as $\gamma\delta$ T cell progenitors or adult HSC (Anderson et al., 2007). Finally, we have shown that Rpl22 loss predisposes T lineage progenitors to transformation through regulation of the NFκB/Lin28B signaling axis (Rao et al., 2012); however, our RNA-Seq analysis revealed no evidence of Lin28B induction, perhaps because Lin28B expression is normally restricted to fetal hematopoiesis (Kristiansen et al., 2016). The basis for the distinct mechanisms of action of Rpl22 in different tissues is unclear, but is likely due to differences in cellular context, resulting either from alterations in the expression, accessibility, or importance of the RNA targets of Rpl22.

The regulation of HSC function and leukemia survival by Rpl22 is dependent on the regulation of Alox12 expression, which Rpl22 controls at the post-transcriptional level. Two modes of action have been proposed to explain how insufficiency of an RNA-binding RP might selectively regulate the expression of proteins encoded by particular mRNA targets: through effects on the ribosome itself or through extraribosomal activity. The manner in which RP insufficiency influences the ribosome remains controversial. The specialized ribosome model suggests that

ribosomes with differing complements of RP exhibit distinct capacities to translate mRNAs bearing specific primary sequence motifs or secondary structural features (Genuth and Barna, 2018b; Kampen et al., 2020; Kang et al., 2021; Shi and Barna, 2015). An opposing model suggests that RP insufficiency attenuates the translation of a selected class of mRNA species because it decreases the number of available ribosomes, rather than by altering their composition (Khajuria et al., 2018). Evidence in support of both models has been reported (Khajuria et al., 2018; Shi et al., 2017). RP can also regulate the activity of mRNA targets when physically separated from the ribosome, or “extra-ribosomally” (Warner and McIntosh, 2009). Strong support exists for this model, including the well documented ability of Rpl13a to dissociate from the ribosome following interferon signaling and to bind to selected mRNA targets, thereby regulating their translation (Jia et al., 2012). Our analysis has not definitively distinguished the mode of action through which Rpl22 regulates Alox12 expression; however, our evidence most closely aligns with the extraribosomal model. Indeed, since Rpl22 appears to assemble into the ribosome as a monomer with a single RNA binding face (Houmani and Ruf, 2009; Klinge et al., 2012), it is capable of binding to either the 28S rRNA required for its assembly into the ribosome, or to an RNA target bearing its recognition motif, but a single Rpl22 molecule is incapable of performing both activities. Accordingly, the ability of Rpl22 to directly bind to *Alox12* mRNA suggests that Rpl22 regulates Alox12 expression by extraribosomal binding to *Alox12* mRNA, and excluding it from polysomes, where it would be translated into protein. Efforts are in progress to define the precise mechanism through which Rpl22 controls the inclusion of *Alox12* mRNA in polysomes.

Our loss of function analysis implicates Alox12 as a critical target through which Rpl22 regulates HSC behavior and the survival of Rpl22-deficient leukemias, in agreement with observations implicating other lipoxygenases in the maintenance of both normal and cancer stem cells. Indeed, loss of function analysis has revealed a requirement for lipoxygenase activity in the maintenance of normal HSC (Kinder et al., 2010). Likewise, lipoxygenase activity has been shown

to be required for the survival of chronic myeloid leukemia stem cells, as well as serving as marker for prostate cancer stem cells (Chen et al., 2014; Yin et al., 2011). These observations support our novel finding that Rpl22 loss enhances HSC self-renewal and facilitates leukemia development and survival through Alox12 induction.

A critical remaining question is how Alox12 induction is able to alter HSC function and promote the survival of the resulting leukemias. Alox12 acts to break down polyunsaturated fatty acids, particularly arachidonic acid, into smaller lipid moieties, including 12S-HETE, which is elevated in Rpl22-deficient HSPC. 12S-HETE serves as activating ligand of the PPAR family of transcriptional regulators (Kuhn et al., 2015; Li et al., 2004). PPARδ has been demonstrated to be a master regulator of FAO (Ito et al., 2012). Activation of PPARδ and FAO by such ligands was also reported to promote asymmetric, self-renewing divisions by HSC (Ito et al., 2012). This is consistent with our observations in Rpl22-deficient HSC, where we observed both the induction of numerous PPARδ targets and increased FAO, which was required for the prolonged retention of a stem cell phenotype by Rpl22-/- HSC, their prolonged ability to form colonies, and for the survival of the resulting leukemias. The colony forming capacity of Rpl22-deficient leukemias was also dependent upon PPARδ, suggesting that the Alox12-PPARδ-FAO axis plays an important role in sustaining survival of Rpl22-deficient leukemias, in agreement with other reports implicating FAO in promoting the survival of subsets of leukemias and leukemia stem cells (German et al., 2016; Stevens et al., 2020; Tabe et al., 2020; Ye et al., 2016).

These and other observations underscore the critical role that alterations in lipid metabolism play in solid and hematologic malignancies, as well as in the control of HSC function (Ito et al., 2012; Keckesova et al., 2017; Schell et al., 2014; Stevens et al., 2020; Vacanti et al., 2014). Nevertheless, the molecular basis by which enhanced FAO supports the function of normal HSC and leukemia cells generally, and specifically in the context of Rpl22 loss, remains to be established. There are three potential non-mutually, exclusive processes that might contribute to

these altered behaviors. First, FAO is capable of generating energy through the contribution of NADH and FADH to the mitochondrial electron transport chain (ETC) to generate ATP (Carracedo et al., 2013). However, *Rpl22-/-* HSPC exhibited a reduction in oxygen consumption rate, a surrogate measure or aerobic respiration, suggesting that the generation of energy was unlikely to be responsible. The reduction in oxygen consumption is likely to result from reduced expression of *ATP5e*, which is important for the consumption of oxygen by ETC complex IV (Mayr et al., 2010). Second, FAO might enhance the survival of *Rpl22-/-* HSPC, since FAO has been reported to modulate the function of Bcl2 family members (Samudio et al., 2010). This could explain how FAO promotes the survival of *Rpl22-/-* leukemias. Finally, FAO also generates substantial quantities of acetyl-CoA, which can enter the Krebs cycle to generate citrate and contribute to NADPH-producing reactions. Alternatively, the acetyl-CoA can be released to the cytosol where it could alter cell behavior through the acetylation of both cytosolic and nuclear proteins (McDonnell et al., 2016; Moussaieff et al., 2015). Indeed, our preliminary proteomic analysis has revealed that Rpl22-deficient leukemias exhibit profound alterations in protein acetylation (data not shown). Efforts are in progress to distinguish among these possibilities.

Taken together, our observations indicate that the RP, Rpl22, employs a novel mode of action to regulate the transformation potential of HSC that does not involve altering global protein synthesis, but is instead focused on the control of cellular lipid metabolism, by regulating the expression of the lipoxygenase, Alox12. Importantly, perturbations in lipid metabolism are increasingly understood to represent therapeutic vulnerabilities in AML (Buettner et al., 2021; Hoang et al., 2022; Jones et al., 2020; Ling et al., 2023; O'Brien et al., 2023; Stevens et al., 2020; Zhang et al., 2022); however, past efforts to pharmacologically attenuate FAO in patients have been limited by liver toxicity (Holubarsch et al., 2007; Jin et al., 2008). Our findings suggest that targeting the lipoxygenases that regulate FAO may represent another fruitful approach, particularly in those patients with *RPL22*-insufficiency.

EXPERIMENTAL PROCEDURES

Competitive transplantation. CD45.1 mice were lethally irradiated with a total dose of 11 Gy, split in two doses of 6.5Gy and 4.5Gy, separated by three hours. After 24 hours, mice were injected retro-orbitally with 300 CD45.2+ LSK/CD48-/CD150+ HSC and 200,000 CD45.1+ competitor bone marrow cells delivered in 200μl Hank's Balanced Salt Solution (HBSS). Engraftment was monitored by retro-orbital bleeding every 4 weeks. Mice were sacrificed after 20 weeks of engraftment and bone marrow was analyzed by flow cytometry.

***In vivo* analysis of protein synthesis.** Protein synthesis by HSC in vivo was measured with OP-Puro, as previously described (Liu et al., 2012; Signer et al., 2014). Mice were injected with 50mg/kg OP-Puro and after one hour the mice were sacrificed and bone marrow was isolated. After lineage reduction, cells were stained with GhostDye710, a fixable live/dead dye (Tonbo Biosciences), and analyzed by flow cytometry using the indicated antibodies. After staining, the cells were fixed and permeabilized using a Fix/Perm kit (BD Biosciences), following which the OP-Puro was conjugated to azide-linked AlexaFluor 488 (Life Technologies) using the Click-It Cell Reaction kit (Life Technologies). Alexa 488 fluorescence was then measured by flow cytometry.

Statistical analysis. A two-tailed student's t-test was used to compare significance between groups in all graphed data. ROUT method was used to identify and confirm clear outliers. Outliers determined by this method are denoted using an asterisk on graphs. Survival-Curves were analyzed using the Mantel-Cox log-rank test. All analyses were performed using Microsoft Excel

or GraphPad Prism Software. P-values, Z-scores, or combined scores associated with gene set enrichment analyses were obtained using the built-in function used by the Enrichr Analysis.

Table S1, related to Figure 4. RNA-Seq analysis of gene expression changes in *Rpl22-/-* HSC.

Table S2, related to Figure 4. Gene ontology (GO) analysis of genes differentially expressed in *Rpl22-/-* HSC.

SUPPLEMENTAL INFORMATION

Supplemental Information includes Supplemental Experimental Procedures, 7 figures, and 3 tables and can be found with this article online

AUTHOR CONTRIBUTIONS

B.H., D.K.S. designed and performed most of the experiments, interpreted data and wrote the manuscript. S.P.F., S.R.S, and S.P. analyzed the RNA-Seq data. M.V., J.P., R.K., O.G., J.B., A.P., K.R., C.M., K.P., M.W., JW, JT, MH, MH, JW, BK, YZ, and U.S. helped with experiments. In collaboration with A.V, and S.S., D.L.W. oversaw the design, execution, and interpretation of the data, and assisted in writing the manuscript.

COMPETING INTERESTS

The authors declare no competing interests.

ACKNOWLEDGEMENTS

This work was supported by NIH grants R37AI110985, P30CA006927, an appropriation from the Commonwealth of Pennsylvania, the Leukemia and Lymphoma Society, and the Bishop Fund. We are grateful to the Wiest laboratory for helpful suggestions and Dr. Avinash Bhandoola, for critical evaluation of the manuscript. These studies were supported by the following core facilities at Fox Chase: Cell Culture, Flow Cytometry, Biostatistics and Bioinformatics, Genomics, DNA Sequencing, and Laboratory Animal.

REFERENCES:

Almeida, M., Ambrogini, E., Han, L., Manolagas, S.C., and Jilka, R.L. (2009). Increased lipid oxidation causes oxidative stress, increased peroxisome proliferator-activated receptor-gamma expression, and diminished pro-osteogenic Wnt signaling in the skeleton. The Journal of biological chemistry *284*, 27438-27448.

Anderson, S.J., Lauritsen, J.P., Hartman, M.G., Foushee, A.M., Lefebvre, J.M., Shinton, S.A., Gerhardt, B., Hardy, R.R., Oravecz, T., and Wiest, D.L. (2007). Ablation of ribosomal protein L22 selectively impairs alphabeta T cell development by activation of a p53-dependent checkpoint. Immunity *26*, 759-772.

Antinozzi, P.A., Segall, L., Prentki, M., McGarry, J.D., and Newgard, C.B. (1998). Molecular or pharmacologic perturbation of the link between glucose and lipid metabolism is without effect on glucose-stimulated insulin secretion. A re-evaluation of the long-chain acyl-CoA hypothesis. The Journal of biological chemistry *273*, 16146-16154.

Auger-Buendia, M.A., Longuet, M., and Tavitian, A. (1979). Kinetic studies on ribosomal proteins assembly in preribosomal particles and ribosomal subunits of mammalian cells. Biochimica et biophysica acta *563*, 113-128.

Barreyro, L., Will, B., Bartholdy, B., Zhou, L., Todorova, T.I., Stanley, R.F., Ben-Neriah, S., Montagna, C., Parekh, S., Pellagatti, A*., et al.* (2012). Overexpression of IL-1 receptor accessory protein in stem and progenitor cells and outcome correlation in AML and MDS. Blood *120*, 1290-1298.

Buettner, R., Nguyen, L.X.T., Morales, C., Chen, M.H., Wu, X., Chen, L.S., Hoang, D.H., Hernandez Vargas, S., Pullarkat, V., Gandhi, V*., et al.* (2021). Targeting the metabolic vulnerability of acute myeloid leukemia blasts with a combination of venetoclax and 8-chloro-adenosine. J Hematol Oncol *14*, 70. doi: 10.1186/s13045-13021-01076-13044.

Carracedo, A., Cantley, L.C., and Pandolfi, P.P. (2013). Cancer metabolism: fatty acid oxidation in the limelight. Nature reviews Cancer *13*, 227-232.

Chen, Y., Peng, C., Abraham, S.A., Shan, Y., Guo, Z., Desouza, N., Cheloni, G., Li, D., Holyoake, T.L., and Li, S. (2014). Arachidonate 15-lipoxygenase is required for chronic myeloid leukemia stem cell survival. The Journal of clinical investigation *124*, 3847-3862.

Corey, S.J., Minden, M.D., Barber, D.L., Kantarjian, H., Wang, J.C., and Schimmer, A.D. (2007). Myelodysplastic syndromes: the complexity of stem-cell diseases. Nature reviews Cancer *7*, 118-129.

Corral, J., Lavenir, I., Impey, H., Warren, A.J., Forster, A., Larson, T.A., Bell, S., McKenzie, A.N., King, G., and Rabbitts, T.H. (1996). An Mll-AF9 fusion gene made by homologous recombination causes acute leukemia in chimeric mice: a method to create fusion oncogenes. Cell *85*, 853-861.

Danilova, N., and Gazda, H.T. (2015). Ribosomopathies: how a common root can cause a tree of pathologies. Disease models & mechanisms *8*, 1013-1026.

De Keersmaecker, K., Sulima, S.O., and Dinman, J.D. (2015). Ribosomopathies and the paradox of cellular hypo- to hyperproliferation. Blood *125*, 1377-1382.

Deisenroth, C., and Zhang, Y. (2010). Ribosome biogenesis surveillance: probing the ribosomal protein-Mdm2-p53 pathway. Oncogene *29*, 4253-4260.

Dobbelstein, M., and Shenk, T. (1995). In vitro selection of RNA ligands for the ribosomal L22 protein associated with Epstein-Barr virus-expressed RNA by using randomized and cDNA-derived RNA libraries. J Virol *69*, 8027-8034.

Elias, H.K., Schinke, C., Bhattacharyya, S., Will, B., Verma, A., and Steidl, U. (2014). Stem cell origin of myelodysplastic syndromes. Oncogene *33*, 5139-5150.

Fahl, S.P., Harris, B., Coffey, F., and Wiest, D.L. (2015). Rpl22 Loss Impairs the Development of B Lymphocytes by Activating a p53-Dependent Checkpoint. J Immunol *194*, 200-209.

Genuth, N.R., and Barna, M. (2018a). The Discovery of Ribosome Heterogeneity and Its Implications for Gene Regulation and Organismal Life. Mol Cell *71*, 364-374.

Genuth, N.R., and Barna, M. (2018b). Heterogeneity and specialized functions of translation machinery: from genes to organisms. Nature reviews Genetics *19*, 431-452.

German, N.J., Yoon, H., Yusuf, R.Z., Murphy, J.P., Finley, L.W., Laurent, G., Haas, W., Satterstrom, F.K., Guarnerio, J., Zaganjor, E.*, et al.* (2016). PHD3 Loss in Cancer Enables Metabolic Reliance on Fatty Acid Oxidation via Deactivation of ACC2. Mol Cell *63*, 1006-1020.

Gerstung, M., Pellagatti, A., Malcovati, L., Giagounidis, A., Porta, M.G., Jadersten, M., Dolatshad, H., Verma, A., Cross, N.C., Vyas, P.*, et al.* (2015). Combining gene mutation with gene expression data improves outcome prediction in myelodysplastic syndromes. Nature communications *6*, 5901.

Grimwade, D., and Hills, R.K. (2009). Independent prognostic factors for AML outcome. Hematology Am Soc Hematol Educ Program, 385-395.

Hoang, D.H., Morales, C., Rodriguez, I.R., Valerio, M., Guo, J., Chen, M.H., Wu, X., Horne, D., Gandhi, V., Chen, L.S.*, et al.* (2022). Synergy of Venetoclax and 8-Chloro-Adenosine in AML: The Interplay of rRNA Inhibition and Fatty Acid Metabolism. Cancers (Basel) *14*, 1446. doi: 1410.3390/cancers14061446.

Holubarsch, C.J., Rohrbach, M., Karrasch, M., Boehm, E., Polonski, L., Ponikowski, P., and Rhein, S. (2007). A double-blind randomized multicentre clinical trial to evaluate the efficacy and safety of two doses of etomoxir in comparison with placebo in patients with moderate congestive heart failure: the ERGO (etomoxir for the recovery of glucose oxidation) study. Clin Sci (Lond) *113*, 205-212.

Horton, S.J., Jaques, J., Woolthuis, C., van Dijk, J., Mesuraca, M., Huls, G., Morrone, G., Vellenga, E., and Schuringa, J.J. (2013). MLL-AF9-mediated immortalization of human hematopoietic cells along different lineages changes during ontogeny. Leukemia *27*, 1116-1126.

Houmani, J.L., and Ruf, I.K. (2009). Clusters of basic amino acids contribute to RNA binding and nucleolar localization of ribosomal protein L22. PLoS ONE *4*, e5306.

Ito, K., Carracedo, A., Weiss, D., Arai, F., Ala, U., Avigan, D.E., Schafer, Z.T., Evans, R.M., Suda, T., Lee, C.H.*, et al.* (2012). A PML-PPAR-delta pathway for fatty acid oxidation regulates hematopoietic stem cell maintenance. Nature medicine *18*, 1350-1358.

Ivanov, A.V., Malygin, A.A., and Karpova, G.G. (2006). [Eukaryotic ribosomal proteins: interaction with their own pre-mRNAs and involvement in the splicing regulation]. Mol Biol (Mosk) *40*, 640-649.

Jia, J., Arif, A., Willard, B., Smith, J.D., Stuehr, D.J., Hazen, S.L., and Fox, P.L. (2012). Protection of extraribosomal RPL13a by GAPDH and dysregulation by S-nitrosylation. Molecular cell *47*, 656-663.

Jin, G., Arai, K., Murata, Y., Wang, S., Stins, M.F., Lo, E.H., and van Leyen, K. (2008). Protecting against cerebrovascular injury: contributions of 12/15-lipoxygenase to edema formation after transient focal ischemia. Stroke *39*, 2538-2543.

Jones, C.L., Stevens, B.M., Pollyea, D.A., Culp-Hill, R., Reisz, J.A., Nemkov, T., Gehrke, S., Gamboni, F., Krug, A., Winters, A.*, et al.* (2020). Nicotinamide Metabolism Mediates Resistance to Venetoclax in Relapsed Acute Myeloid Leukemia Stem Cells. Cell Stem Cell *27*, 748-764.e744. doi: 710.1016/j.stem.2020.1007.1021. Epub 2020 Aug 1020.

Kampen, K.R., Sulima, S.O., Vereecke, S., and De Keersmaecker, K. (2020). Hallmarks of ribosomopathies. Nucleic Acids Res *48*, 1013-1028. doi: 1010.1093/nar/gkz1637.

Kang, J., Brajanovski, N., Chan, K.T., Xuan, J., Pearson, R.B., and Sanij, E. (2021). Ribosomal proteins and human diseases: molecular mechanisms and targeted therapy. Signal Transduct Target Ther *6*, 323. doi: 310.1038/s41392-41021-00728-41398.

Keckesova, Z., Donaher, J.L., De Cock, J., Freinkman, E., Lingrell, S., Bachovchin, D.A., Bierie, B., Tischler, V., Noske, A., Okondo, M.C*., et al.* (2017). LACTB is a tumour suppressor that modulates lipid metabolism and cell state. Nature *543*, 681-686.

Khajuria, R.K., Munschauer, M., Ulirsch, J.C., Fiorini, C., Ludwig, L.S., McFarland, S.K., Abdulhay, N.J., Specht, H., Keshishian, H., Mani, D.R*., et al.* (2018). Ribosome Levels Selectively Regulate Translation and Lineage Commitment in Human Hematopoiesis. Cell *173*, 90-103.e119.

Kiel, M.J., Yilmaz, O.H., Iwashita, T., Yilmaz, O.H., Terhorst, C., and Morrison, S.J. (2005). SLAM family receptors distinguish hematopoietic stem and progenitor cells and reveal endothelial niches for stem cells. Cell *121*, 1109-1121.

Kinder, M., Wei, C., Shelat, S.G., Kundu, M., Zhao, L., Blair, I.A., and Pure, E. (2010). Hematopoietic stem cell function requires 12/15-lipoxygenase-dependent fatty acid metabolism. Blood *115*, 5012-5022.

Klinge, S., Voigts-Hoffmann, F., Leibundgut, M., and Ban, N. (2012). Atomic structures of the eukaryotic ribosome. Trends Biochem Sci *37*, 189-198.

Kondrashov, N., Pusic, A., Stumpf, C.R., Shimizu, K., Hsieh, A.C., Xue, S., Ishijima, J., Shiroishi, T., and Barna, M. (2011). Ribosome-mediated specificity in Hox mRNA translation and vertebrate tissue patterning. Cell *145*, 383-397.

Kristiansen, T.A., Jaensson Gyllenback, E., Zriwil, A., Bjorklund, T., Daniel, J.A., Sitnicka, E., Soneji, S., Bryder, D., and Yuan, J. (2016). Cellular Barcoding Links B-1a B Cell Potential to a Fetal Hematopoietic Stem Cell State at the Single-Cell Level. Immunity *45*, 346-357.

Kuhn, H., Banthiya, S., and van Leyen, K. (2015). Mammalian lipoxygenases and their biological relevance. Biochimica et biophysica acta *1851*, 308-330.

Kuhn, R., Schwenk, F., Aguet, M., and Rajewsky, K. (1995). Inducible gene targeting in mice. Science *269*, 1427-1429.

Lapidot, T., Sirard, C., Vormoor, J., Murdoch, B., Hoang, T., Caceres-Cortes, J., Minden, M., Paterson, B., Caligiuri, M.A., and Dick, J.E. (1994). A cell initiating human acute myeloid leukaemia after transplantation into SCID mice. Nature *367*, 645-648.

Li, Q., Cheon, Y.P., Kannan, A., Shanker, S., Bagchi, I.C., and Bagchi, M.K. (2004). A novel pathway involving progesterone receptor, 12/15-lipoxygenase-derived eicosanoids, and peroxisome proliferator-activated receptor gamma regulates implantation in mice. The Journal of biological chemistry *279*, 11570-11581.

Ling, Q., Mao, S., Pan, J., Wei, W., Qian, Y., Li, F., Huang, S., Ye, W., Lin, X., Huang, J*., et al.* (2023). CPT1B, a metabolic molecule, is also an independent risk factor in CN-AML. Cancer Biomark *6*, CBM-210043.

Linman, J.W., and Bagby, C., Jr. (1976). The preleukemic syndrome: clinical and laboratory features, natural course, and management. Nouv Rev Fr Hematol Blood Cells *17*, 11-31.

Liu, J., Xu, Y., Stoleru, D., and Salic, A. (2012). Imaging protein synthesis in cells and tissues with an alkyne analog of puromycin. Proc Natl Acad Sci U S A *109*, 413-418.

Lyublinskaya, O.G., Borisov, Y.G., Pugovkina, N.A., Smirnova, I.S., Obidina, J.V., Ivanova, J.S., Zenin, V.V., Shatrova, A.N., Borodkina, A.V., Aksenov, N.D*., et al.* (2015). Reactive Oxygen Species Are Required for Human Mesenchymal Stem Cells to Initiate Proliferation after the Quiescence Exit. Oxid Med Cell Longev *2015*, 502105.

Mayr, J.A., Havlickova, V., Zimmermann, F., Magler, I., Kaplanova, V., Jesina, P., Pecinova, A., Nuskova, H., Koch, J., Sperl, W*., et al.* (2010). Mitochondrial ATP synthase deficiency due to a mutation in the ATP5E gene for the F1 epsilon subunit. Human molecular genetics *19*, 3430-3439.

McDonnell, E., Crown, S.B., Fox, D.B., Kitir, B., Ilkayeva, O.R., Olsen, C.A., Grimsrud, P.A., and Hirschey, M.D. (2016). Lipids Reprogram Metabolism to Become a Major Carbon Source for Histone Acetylation. Cell reports *17*, 1463-1472.

Miraki-Moud, F., Anjos-Afonso, F., Hodby, K.A., Griessinger, E., Rosignoli, G., Lillington, D., Jia, L., Davies, J.K., Cavenagh, J., Smith, M.*, et al.* (2013). Acute myeloid leukemia does not deplete normal hematopoietic stem cells but induces cytopenias by impeding their differentiation. Proc Natl Acad Sci U S A *110*, 13576-13581.

Moussaieff, A., Rouleau, M., Kitsberg, D., Cohen, M., Levy, G., Barasch, D., Nemirovski, A., Shen-Orr, S., Laevsky, I., Amit, M.*, et al.* (2015). Glycolysis-mediated changes in acetyl-CoA and histone acetylation control the early differentiation of embryonic stem cells. Cell Metab *21*, 392-402.

Nakhoul, H., Ke, J., Zhou, X., Liao, W., Zeng, S.X., and Lu, H. (2014). Ribosomopathies: mechanisms of disease. Clin Med Insights Blood Disord *7*, 7-16.

Narla, A., and Ebert, B.L. (2010). Ribosomopathies: human disorders of ribosome dysfunction. Blood *115*, 3196-3205.

Norris, K., Hopes, T., and Aspden, J.L. (2021). Ribosome heterogeneity and specialization in development. Wiley Interdiscip Rev RNA *12*, e1644. doi: 1610.1002/wrna.1644. Epub 2021 Feb 1649.

O'Brien, C., Ling, T., Berman, J.M., Culp-Hill, R., Reisz, J.A., Rondeau, V., Jahangiri, S., St-Germain, J., Macwan, V., Astori, A.*, et al.* (2023). Simultaneous inhibition of Sirtuin 3 and cholesterol homeostasis targets acute myeloid leukemia stem cells by perturbing fatty acid β-oxidation and inducing lipotoxicity. Haematologica *6*, 281894.

O'Leary, M.N., Schreiber, K.H., Zhang, Y., Duc, A.C., Rao, S., Hale, J.S., Academia, E.C., Shah, S.R., Morton, J.F., Holstein, C.A.*, et al.* (2013). The ribosomal protein Rpl22 controls ribosome composition by directly repressing expression of its own paralog, Rpl22l1. PLoS Genet *9*, e1003708.

Oguro, H., Ding, L., and Morrison, S.J. (2013). SLAM family markers resolve functionally distinct subpopulations of hematopoietic stem cells and multipotent progenitors. Cell Stem Cell *13*, 102-116.

Rao, S., Lee, S.Y., Gutierrez, A., Perrigoue, J., Thapa, R.J., Tu, Z., Jeffers, J.R., Rhodes, M., Anderson, S., Oravecz, T.*, et al.* (2012). Inactivation of ribosomal protein L22 promotes transformation by induction of the stemness factor, Lin28B. Blood *120*, 3764-3773.

Samudio, I., Harmancey, R., Fiegl, M., Kantarjian, H., Konopleva, M., Korchin, B., Kaluarachchi, K., Bornmann, W., Duvvuri, S., Taegtmeyer, H.*, et al.* (2010). Pharmacologic inhibition of fatty acid oxidation sensitizes human leukemia cells to apoptosis induction. J Clin Invest *120*, 142-156.

Sanz, E., Yang, L., Su, T., Morris, D.R., McKnight, G.S., and Amieux, P.S. (2009). Cell-type-specific isolation of ribosome-associated mRNA from complex tissues. Proc Natl Acad Sci U S A *106*, 13939-13944.

Saultz, J.N., and Garzon, R. (2016). Acute Myeloid Leukemia: A Concise Review. Journal of clinical medicine *5*.

Schell, J.C., Olson, K.A., Jiang, L., Hawkins, A.J., Van Vranken, J.G., Xie, J., Egnatchik, R.A., Earl, E.G., DeBerardinis, R.J., and Rutter, J. (2014). A role for the mitochondrial pyruvate carrier as a repressor of the Warburg effect and colon cancer cell growth. Mol Cell *56*, 400-413.

Schneider, R.K., Schenone, M., Ferreira, M.V., Kramann, R., Joyce, C.E., Hartigan, C., Beier, F., Brummendorf, T.H., Germing, U., Platzbecker, U.*, et al.* (2016). Rps14 haploinsufficiency causes a block in erythroid differentiation mediated by S100A8 and S100A9. Nat Med *22*, 288-297.

Shi, Z., and Barna, M. (2015). Translating the genome in time and space: specialized ribosomes, RNA regulons, and RNA-binding proteins. Annual review of cell and developmental biology *31*, 31-54.

Shi, Z., Fujii, K., Kovary, K.M., Genuth, N.R., Rost, H.L., Teruel, M.N., and Barna, M. (2017). Heterogeneous Ribosomes Preferentially Translate Distinct Subpools of mRNAs Genome-wide. Mol Cell *67*, 71-83.e77.

Signer, R.A., Magee, J.A., Salic, A., and Morrison, S.J. (2014). Haematopoietic stem cells require a highly regulated protein synthesis rate. Nature *509*, 49-54.

Singbrant, S., Karlsson, G., Ehinger, M., Olsson, K., Jaako, P., Miharada, K., Stadtfeld, M., Graf, T., and Karlsson, S. (2010). Canonical BMP signaling is dispensable for hematopoietic stem cell function in both adult and fetal liver hematopoiesis, but essential to preserve colon architecture. Blood *115*, 4689-4698.

Singh, D., Chang, S.J., Lin, P.H., Averina, O.V., Kaberdin, V.R., and Lin-Chao, S. (2009). Regulation of ribonuclease E activity by the L4 ribosomal protein of Escherichia coli. Proc Natl Acad Sci U S A *106*, 864-869.

Solanki, N.R., Stadanlick, J.E., Zhang, Y., Duc, A.C., Lee, S.Y., Lauritsen, J.P., Zhang, Z., and Wiest, D.L. (2016). Rpl22 Loss Selectively Impairs alphabeta T Cell Development by Dysregulating Endoplasmic Reticulum Stress Signaling. Journal of immunology (Baltimore, Md : 1950) *197*, 2280-2289.

Stevens, B.M., Jones, C.L., Pollyea, D.A., Culp-Hill, R., D'Alessandro, A., Winters, A., Krug, A., Abbott, D., Goosman, M., Pei, S.*, et al.* (2020). Fatty acid metabolism underlies venetoclax resistance in acute myeloid leukemia stem cells. Nat Cancer *1*, 1176-1187. doi: 1110.1038/s43018-43020-00126-z. Epub 42020 Oct 43026.

Sulima, S.O., Kampen, K.R., and De Keersmaecker, K. (2019). Cancer Biogenesis in Ribosomopathies. Cells *8*, 229. doi: 210.3390/cells8030229.

Sun, D., and Funk, C.D. (1996). Disruption of 12/15-lipoxygenase expression in peritoneal macrophages. Enhanced utilization of the 5-lipoxygenase pathway and diminished oxidation of low density lipoprotein. J Biol Chem *271*, 24055-24062.

Tabe, Y., Konopleva, M., and Andreeff, M. (2020). Fatty Acid Metabolism, Bone Marrow Adipocytes, and AML. Front Oncol *10:155.*, 10.3389/fonc.2020.00155. eCollection 02020.

Taghon, T., Yui, M.A., Pant, R., Diamond, R.A., and Rothenberg, E.V. (2006). Developmental and molecular characterization of emerging beta- and gammadelta-selected pre-T cells in the adult mouse thymus. Immunity *24*, 53-64.

Teng, T., Mercer, C.A., Hexley, P., Thomas, G., and Fumagalli, S. (2013). Loss of tumor suppressor RPL5/RPL11 does not induce cell cycle arrest but impedes proliferation due to reduced ribosome content and translation capacity. Mol Cell Biol *33*, 4660-4671.

Tutwiler, G.F., Brentzel, H.J., and Kiorpes, T.C. (1985). Inhibition of mitochondrial carnitine palmitoyl transferase A in vivo with methyl 2-tetradecylglycidate (methyl palmoxirate) and its relationship to ketonemia and glycemia. Proc Soc Exp Biol Med *178*, 288-296.

Tyner, J.W., Tognon, C.E., Bottomly, D., Wilmot, B., Kurtz, S.E., Savage, S.L., Long, N., Schultz, A.R., Traer, E., Abel, M.*, et al.* (2018). Functional genomic landscape of acute myeloid leukaemia. Nature *562*, 526-531.

Vacanti, N.M., Divakaruni, A.S., Green, C.R., Parker, S.J., Henry, R.R., Ciaraldi, T.P., Murphy, A.N., and Metallo, C.M. (2014). Regulation of substrate utilization by the mitochondrial pyruvate carrier. Mol Cell *56*, 425-435.

Warner, J.K., Wang, J.C., Hope, K.J., Jin, L., and Dick, J.E. (2004). Concepts of human leukemic development. Oncogene *23*, 7164-7177.

Warner, J.R., and McIntosh, K.B. (2009). How common are extraribosomal functions of ribosomal proteins? Mol Cell *34*, 3-11.

Will, B., Zhou, L., Vogler, T.O., Ben-Neriah, S., Schinke, C., Tamari, R., Yu, Y., Bhagat, T.D., Bhattacharyya, S., Barreyro, L.*, et al.* (2012). Stem and progenitor cells in myelodysplastic syndromes show aberrant stage-specific expansion and harbor genetic and epigenetic alterations. Blood *120*, 2076-2086.

Woll, P.S., Kjallquist, U., Chowdhury, O., Doolittle, H., Wedge, D.C., Thongjuea, S., Erlandsson, R., Ngara, M., Anderson, K., Deng, Q.*, et al.* (2014). Myelodysplastic syndromes are propagated by rare and distinct human cancer stem cells in vivo. Cancer cell *25*, 794-808.

Ye, H., Adane, B., Khan, N., Sullivan, T., Minhajuddin, M., Gasparetto, M., Stevens, B., Pei, S., Balys, M., Ashton, J.M.*, et al.* (2016). Leukemic Stem Cells Evade Chemotherapy by Metabolic Adaptation to an Adipose Tissue Niche. Cell Stem Cell *19*, 23-37.

Yin, B., Yang, Y., Zhao, Z., Zeng, Y., Mooney, S.M., Li, M., Xu, X., Song, Y., Wu, B., and Yang, Z. (2011). Arachidonate 12-lipoxygenase may serve as a potential marker and therapeutic target for prostate cancer stem cells. International journal of oncology *38*, 1041-1046.

Zhang, Y., Duc, A.C., Rao, S., Sun, X.L., Bilbee, A.N., Rhodes, M., Li, Q., Kappes, D.J., Rhodes, J., and Wiest, D.L. (2013). Control of hematopoietic stem cell emergence by antagonistic functions of ribosomal protein paralogs. Dev Cell *24*, 411-425.

Zhang, Y., O'Leary, M.N., Peri, S., Wang, M., Zha, J., Melov, S., Kappes, D.J., Feng, Q., Rhodes, J., Amieux, P.S.*, et al.* (2017). Ribosomal Proteins Rpl22 and Rpl22l1 Control Morphogenesis by Regulating Pre-mRNA Splicing. Cell reports *18*, 545-556.

Zhang, Y., Shen, Y., Wei, W., Wang, W., Jiang, D., Ren, Y., Peng, Z., Fan, Q., Cheng, J., and Ma, J. (2022). Dysregulation of SIRT3 SUMOylation Confers AML Chemoresistance via Controlling HES1-Dependent Fatty Acid Oxidation. Int J Mol Sci *23*, 8282. doi: 8210.3390/ijms23158282.

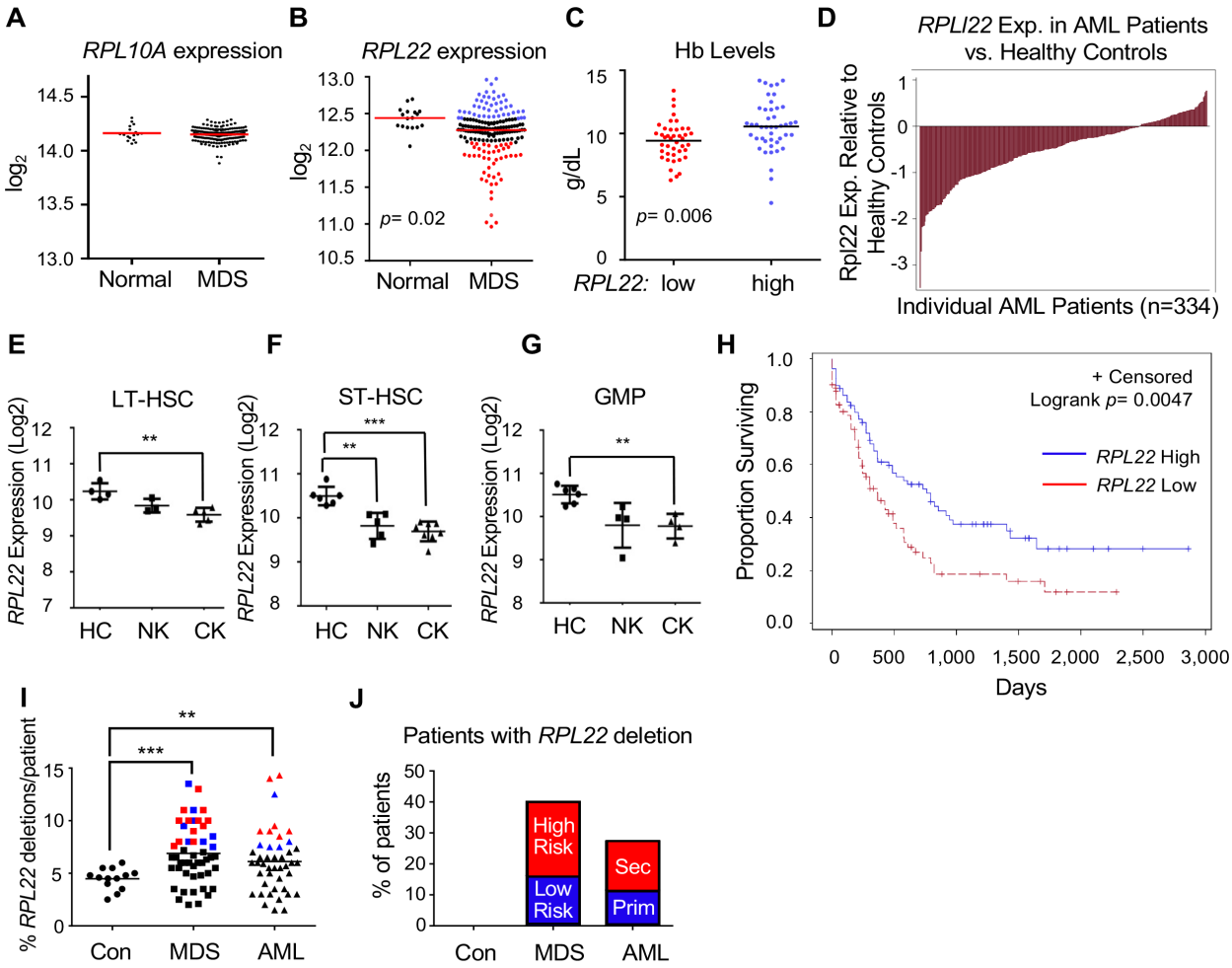

Fig. 1: Reduced *RPL22* expression correlates with more severe MDS and AML. (A-B) Expression levels of *RPL10A* and *RPL22* mRNA *in* CD34+ cells from MDS patients (*n*=183). **(C)** Hemoglobin (Hb) levels of MDS patients with low (bottom quartile) or high (top quartile) *RPL22* expression. **(D)** Waterfall plot of *RPL22* expression in leukocytes from AML patients and healthy controls enrolled in the Beat AML consortium. **(E-G)** *RPL22* mRNA levels in sorted **(E)** LT-HSC (Lin$^-$, CD34+, CD38-, CD90+), **(F)** ST-HSC (Lin-, CD34+, CD38-, CD90-), and **(G)** GMP (Lin-, CD34+, CD38+, CD123+, CD45RA+) from AML bone marrow samples (n=12) compared to age-matched healthy controls (HC; n=4)). Cytogenetic abnormalities are depicted as NK (Normal Karyotype) or CK (Complex Karyotype). **(H)** Graph of survival of AML patients from the TCGA database, with patients with low *RPL22* expression (bottom quartile) compared to those with high expression (top quartile). The survival curve was analyzed for significance using the Mantel-Cox log-rank test. **(I-J)** FISH analysis of deletion of the *RPL22* locus in bone marrow cells from 85 MDS and AML patients. **(I)** Dot-plot representing the fraction of CD34+ cells in which the *RPL22* locus was deleted. Patients in which the frequency of *RPL22* deletion is 3 S.D. greater than the mean of healthy controls are colored, with blue and red colors representing low and high risk MDS, respectively (middle), or primary and secondary AML, respectively (right). **(J)** The distribution of patients with a frequency of *RPL22* deletions greater than 3 S.D. of control were subdivided into low and high risk MDS, and primary and secondary AML, and represented graphically. All graphs were analyzed for significance using the student's t-test, unless otherwise specified. Error bars represent s.e.m. $^{**}p \leq 0.01$, $^{***}p \leq 0.001$.

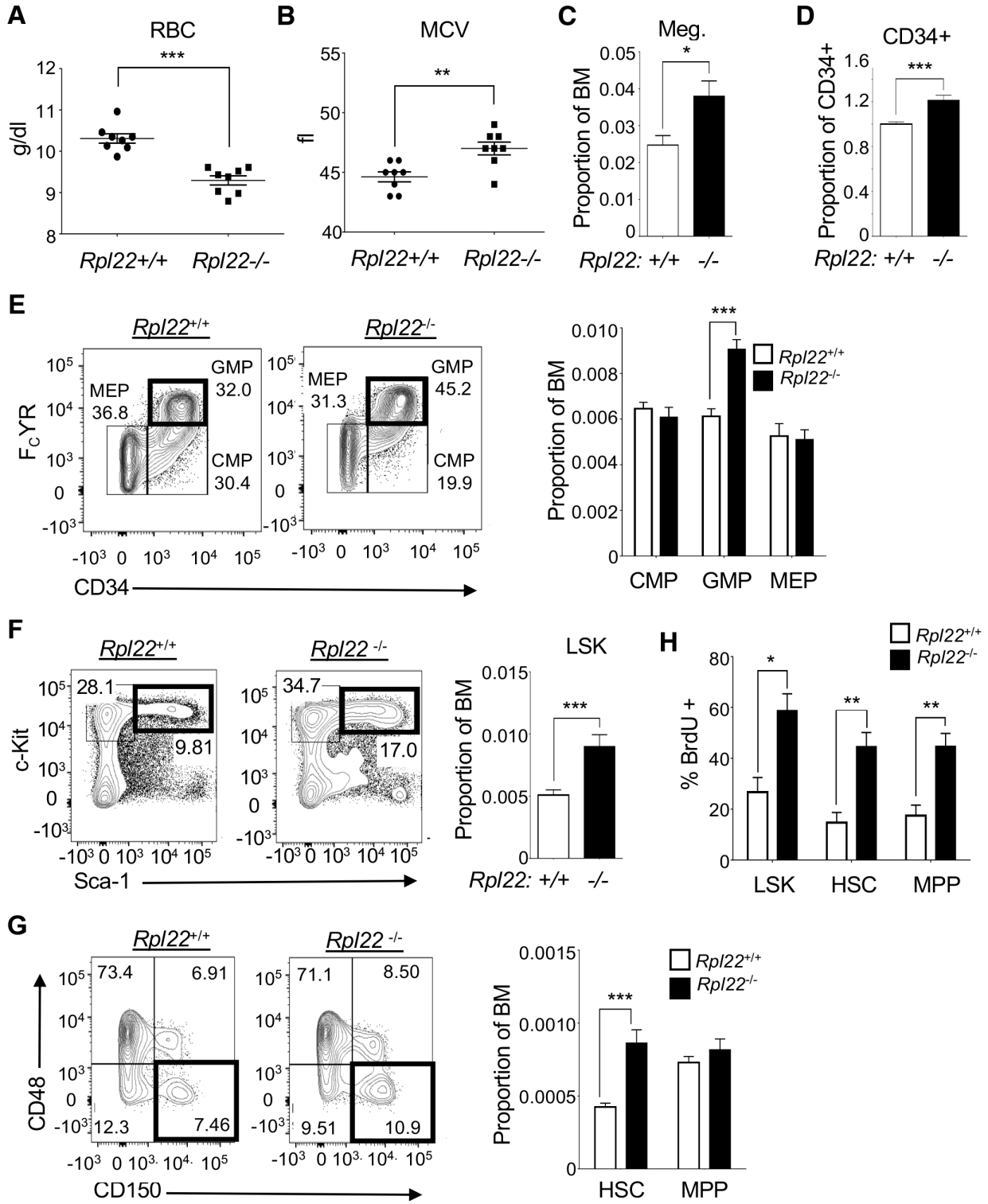

Fig. 2: Rpl22-deficient mice exhibit MDS-like characteristics. (A) Measurement of red blood cells (RBC; g/dL) in the peripheral blood of *Rpl22*$^{-/-}$ and *Rpl22*$^{+/+}$ mice (*n* = 8). **(B)** Measurement of the mean corpuscular volume (MCV) of RBC from *Rpl22*$^{-/-}$ and *Rpl22*$^{+/+}$ mice (*n* = 8). **(C-D)** The proportion of CD41+, FSC-high megakaryocytes (*n* = 9) and CD34+ progenitors (*n* = 18) in the bone marrow of *Rpl22-/-* and *Rpl22+/+* mice was measured by flow cytometry. **(E)** Representative

histograms of Lineage- cKit+ (LK) subsets, defined by FcγR and CD34 (including granulocyte-macrophage progenitors, GMP; LK/CD34+/FcγR high) in the bone marrow of *Rpl22*-/- and *Rpl22*$^{+/+}$ mice. Proportions of the indicated populations are represented graphically on the right +/- standard error (n = 9). **(F-G)** Representative histograms of LSK and HSC (LSK/CD150+/CD48-) in the bone marrow of *Rpl22*$^{-/-}$ and *Rpl22*$^{+/+}$ mice. The proportions are represented graphically as the mean +/- standard error (n = 15). **(H)** Graphical representation of flow cytometric analysis of BrdU incorporation in LSK, HSC, and MPP. (n = 4). All graphs were analyzed for significance using the student's t-test, unless otherwise specified. Error bars represent s.e.m. *$p \leq 0.05$, **$p \leq 0.01$, ***$p \leq 0.001$.

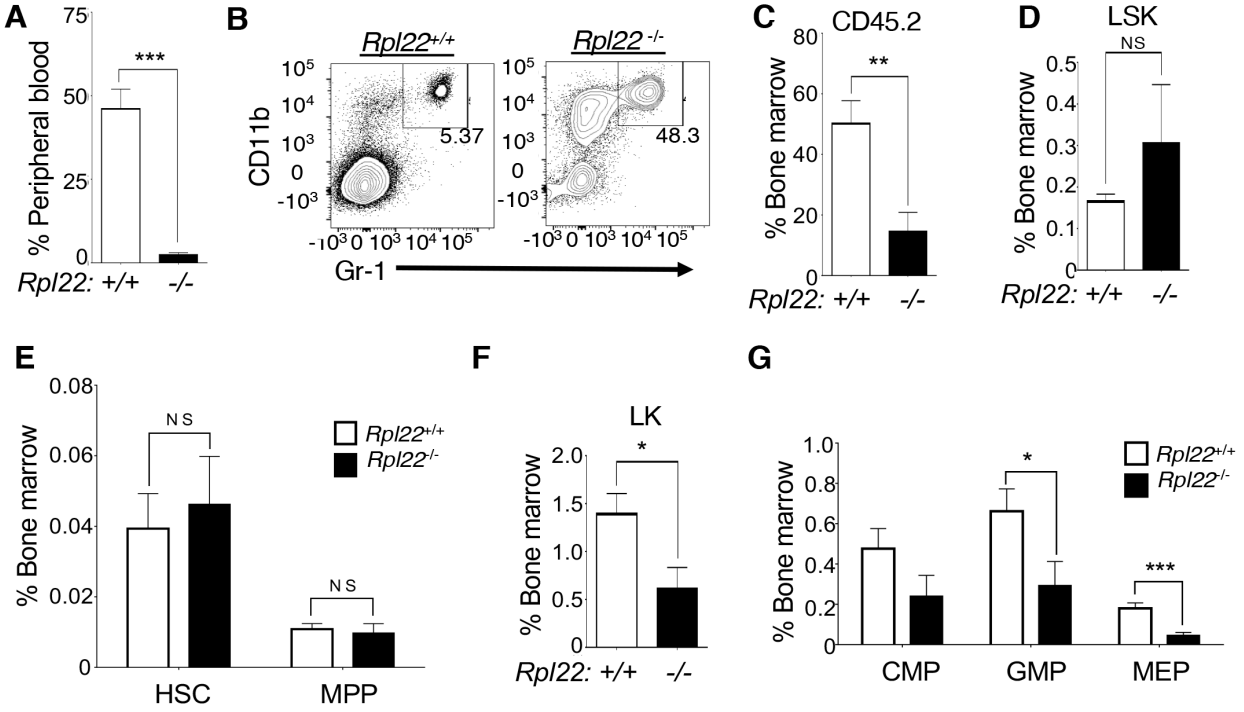

Fig. 3: HSC from Rpl22-deficient mice display altered stem cell function. (A-G) Competitive transplantation of 300 CD45.2 HSC with 200,000 CD45.1 competitor WBM cells. All data shown represent analysis at 20 weeks post-transplantation (n = 10). **(A)** Contribution of CD45.2 *Rpl22+/+* and *Rpl22-/-* HSC to the peripheral blood following competitive transplantation. **(B)** Representative histogram of myeloid lineage cells in the peripheral blood of transplanted mice. **(C-G)** Contribution of CD45.2 *Rpl22+/+* and *Rpl22-/-* HSC to the following bone marrow populations after competitive transplantation: **(C)** total bone marrow cellularity; **(D)** LSK; **(E)** HSC and MPP; **(F)** LK; and **(G)** LK subsets, CMP, GMP, and MEP. All graphs were analyzed for significance using the student's t-test. Error bars represent standard error of the mean (SEM). *$p \leq 0.05$, **$p \leq 0.01$, ***$p \leq 0.001$.

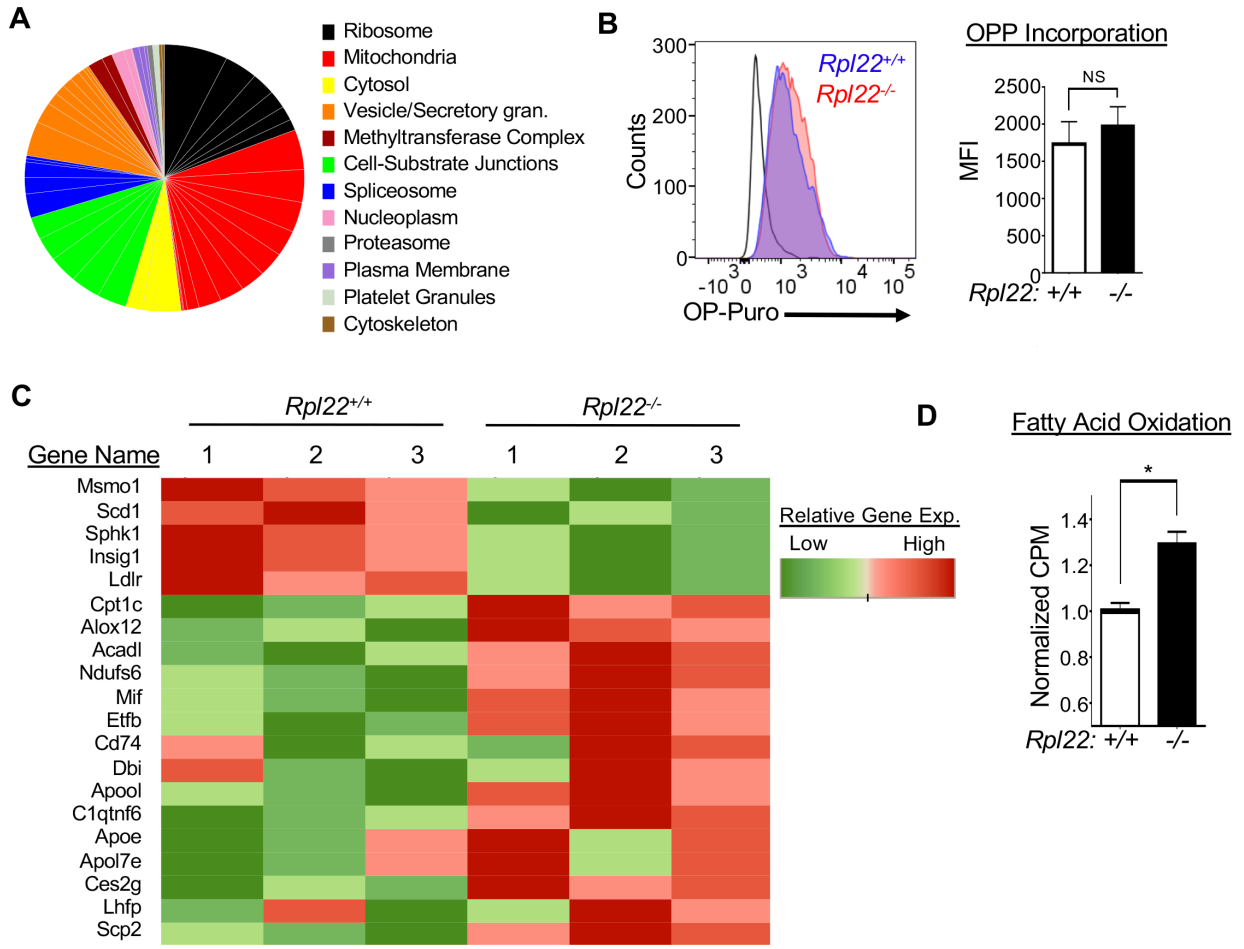

Fig. 4: Rpl22-deficiency changes HSC metabolism, but does not alter global protein synthesis. **(A)** Gene ontology (GO) analysis of genes differentially expressed by *Rpl22*-/- HSC. The differentially expressed genes were identified by RNA-Seq and subjected to GO analysis using the GO Cellular Components Database. Significant gene sets were categorized and represented as a pie chart with the size of the wedges reflecting the EnrichR combined score for a given GO category. **(B)** Protein synthesis was measured in HSC by assessing the amount O-propargyl-puromycin (OPP) incorporated into nascent polypeptides by flow cytometry after exposure to OPP for 1h. A representative FACS histogram of OPP incorporation by HSC is depicted and expressed graphically as the mean +/- SEM of the mean fluorescence intensity (MFI). **(C)** Heat map depicting the expression levels in HSC of genes involved in fatty acid metabolism (n = 3). **(D)** Measurement of fatty acid oxidation (FAO) in *Rpl22*-/- and *Rpl22*+/+ LSK. FAO activity is depicted graphically as the mean +/- SEM of triplicate measurements. All graphs were analyzed for significance using the student's t-test. *$p \leq 0.05$

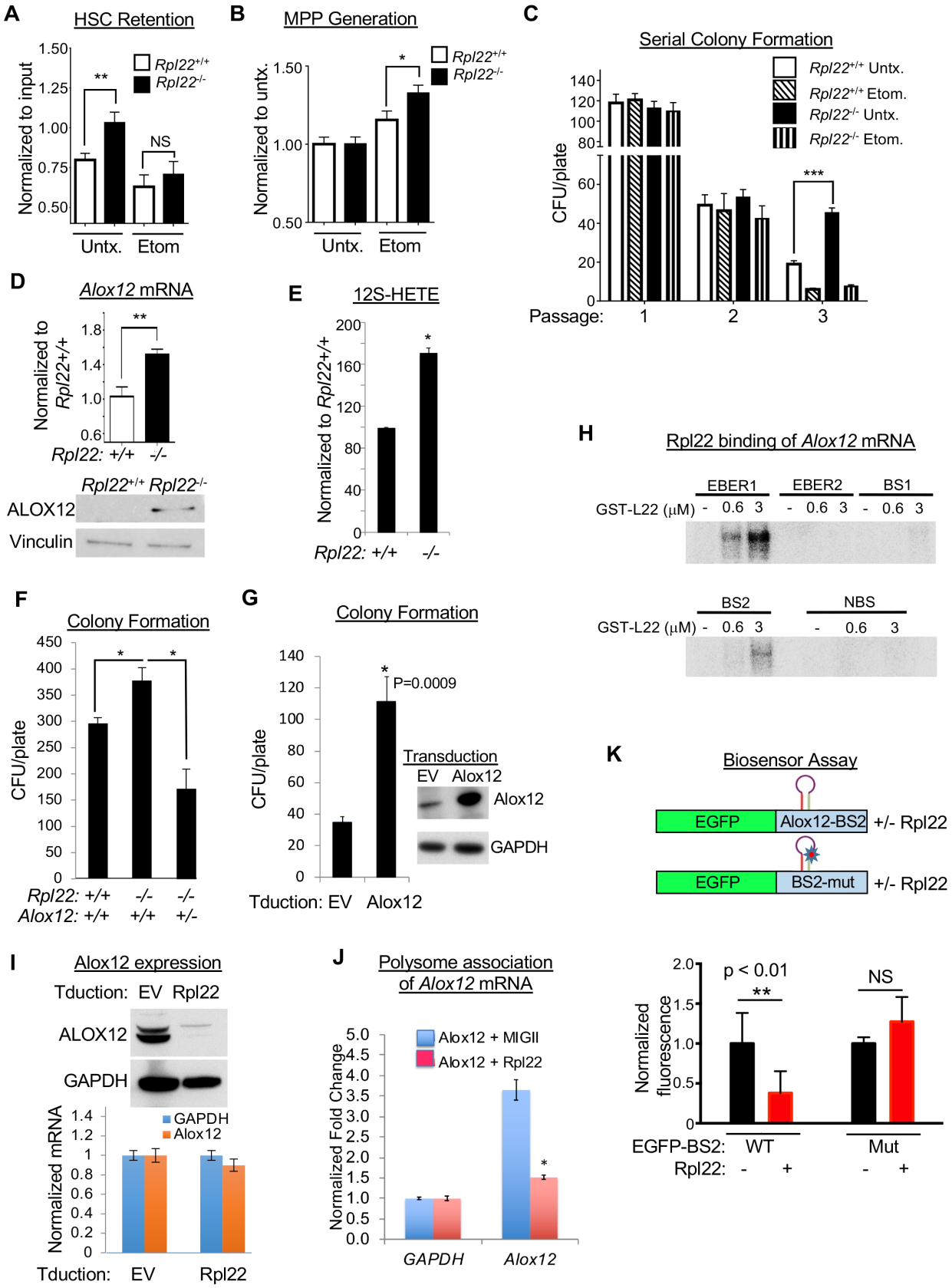
A
HSC Retention
Normalized to input
1.50
1.25
1.00
0.75
0.50
**
NS
Rpl22+/+
Rpl22-/-
Untx.
Etom
B
MPP Generation
Normalized to untx.
1.50
1.00
0.50
*
Rpl22+/+
Rpl22-/-
Untx.
Etom
C
Serial Colony Formation
CFU/plate
140
120
100
80
60
40
20
0
***
Rpl22+/+ Untx.
Rpl22+/+ Etom.
Rpl22-/- Untx.
Rpl22-/- Etom.
Passage: 1 2 3
D
Alox12 mRNA
Normalized to Rpl22+/+
1.8
1.4
1.0
0.6
**
Rpl22: +/+ -/-
Rpl22+/+ Rpl22-/-
ALOX12
Vinculin
E
12S-HETE
Normalized to Rpl22+/+
200
160
120
80
40
0
*
Rpl22: +/+ -/-
H
Rpl22 binding of Alox12 mRNA
EBER1
EBER2
BS1
GST-L22 (μM) - 0.6 3 - 0.6 3 - 0.6 3
BS2
NBS
GST-L22 (μM) - 0.6 3 - 0.6 3
F
Colony Formation
CFU/plate
450
400
350
300
250
200
150
100
50
0
*
*
Rpl22: +/+ -/- -/-
Alox12: +/+ +/+ +/-
G
Colony Formation
CFU/plate
140
120
100
80
60
40
20
0
*
P=0.0009
Transduction
EV Alox12
Alox12
GAPDH
Tduction: EV Alox12
K
Biosensor Assay
EGFP
Alox12-BS2
+/- Rpl22
EGFP
BS2-mut
+/- Rpl22
I
Alox12 expression
Tduction: EV Rpl22
ALOX12
GAPDH
Normalized mRNA
1.4
1.2
1
0.8
0.6
0.4
0.2
0
GAPDH
Alox12
Tduction: EV Rpl22
J
Polysome association of Alox12 mRNA
Normalized Fold Change
5.0
4.5
4.0
3.5
3.0
2.5
2.0
1.5
1.0
0.5
0.0
Alox12 + MIGII
Alox12 + Rpl22
*
GAPDH
Alox12
Normalized fluorescence
2.0
1.5
1.0
0.5
0
p < 0.01
**
NS
EGFP-BS2: WT Mut
Rpl22: - + - +

Fig. 5: The enhanced retention of progenitor activity by Rpl22-deficient HSPC depends on FAO. (A-B) Flow cytometric assessment of the retention of the HSC immunophenotype (CD150+CD48-) or differentiation into MPP following two days of culture in methylcellulose in the presence or absence of 200μM Etomoxir (*n* = 9). **(C)** Serial colony forming ability of *Rpl22-/-* and *Rpl22+/+* HSPCs treated with vehicle (DMSO) or Etomoxir. Mean +/- SEM of colonies of triplicate cultures serially passaged three times is depicted graphically. **(D)** Q-PCR and Immunoblot analysis of *Alox12* mRNA and protein expression, respectively, in *Rpl22+/+* and *Rpl22-/-* HSC and LSK. Triplicate qRT-PCR measurements are represented graphically as mean +/- SEM, with the expression level in *Rpl22-/-* HSC normalized to that in *Rpl22+/+* HSC (n=3). Vinculin was used as an immunoblotting loading control. **(E)** The levels of 12S-HETE in *Rpl22+/+* and *Rpl22-/-* LSK were measured in triplicate by ELISA. The mean level +/- SEM was normalized to that in *Rpl22+/+* LSK and depicted graphically. **(F)** Effect of *Alox12* insufficiency on the colony forming ability of *Rpl22-/-* LSK. Colony-formation by LSK isolated from mice of the indicated genotypes was assessed as in **(C). (G)** The effect of Alox12 overexpression on colony formation by *Rpl22+/+* LSK. *Rpl22+/+* LSK were lentivirally transduced with *Alox12* or an empty vector (EV) control following which their colony forming capacity was assessed as in **(C). (H)** Assessment of GST-Rpl22 binding to the indicated fragments of *Alox12* mRNA (BS1, binding site 1; BS2, binding site 2; and NBS, non-binding site) as measured by EMSA analysis. *EBER1* and *EBER2* RNA served as positive and negative controls, respectively. **(I)** Repression of Alox12 expression by Rpl22. *Rpl22-/-* MEF ectopically expressing the coding region of murine *Alox12* were transduced with either the empty vector (EV) control or pMiG-Rpl22, following which the effect on Alox12 expression was assessed by immunoblotting and qRT-PCR as in **(D). (J)** Control of *Alox12* mRNA inclusion in polysomes. Cells from **(I)** were fractionated on a continuous sucrose gradient, which separated cellular RNA into polysome-associated and free fractions. The amount of free and polysome associated *Alox12* and *Gapdh* RNA was quantified by qRT-PCR, and normalized to that in the EV transduced control, as in **(I)**. **(K)** Transfer of Rpl22-responsiveness to mRNA encoding GFP using the Rpl22-binding site in *Alox12* mRNA. *Gfp*-constructs appended in-frame with intact or mutated *Alox12* BS2 were injected into zebrafish embryos at the 1 cell stage alone or with mRNA encoding Rpl22 **(Fig. S6G)**. After 10h, GFP fluorescence was quantified and depicted graphically after normalization to the fluorescence intensity of the intact BS2 construct in control injected fish. All data are representative of 3 experiments performed, unless otherwise stated. All graphs were analyzed for significance using the student's t-test. Error bars represent standard error of the mean (SEM). $^{*}p \leq 0.05$, $^{**}p \leq 0.01$, $^{***}p \leq 0.001$.

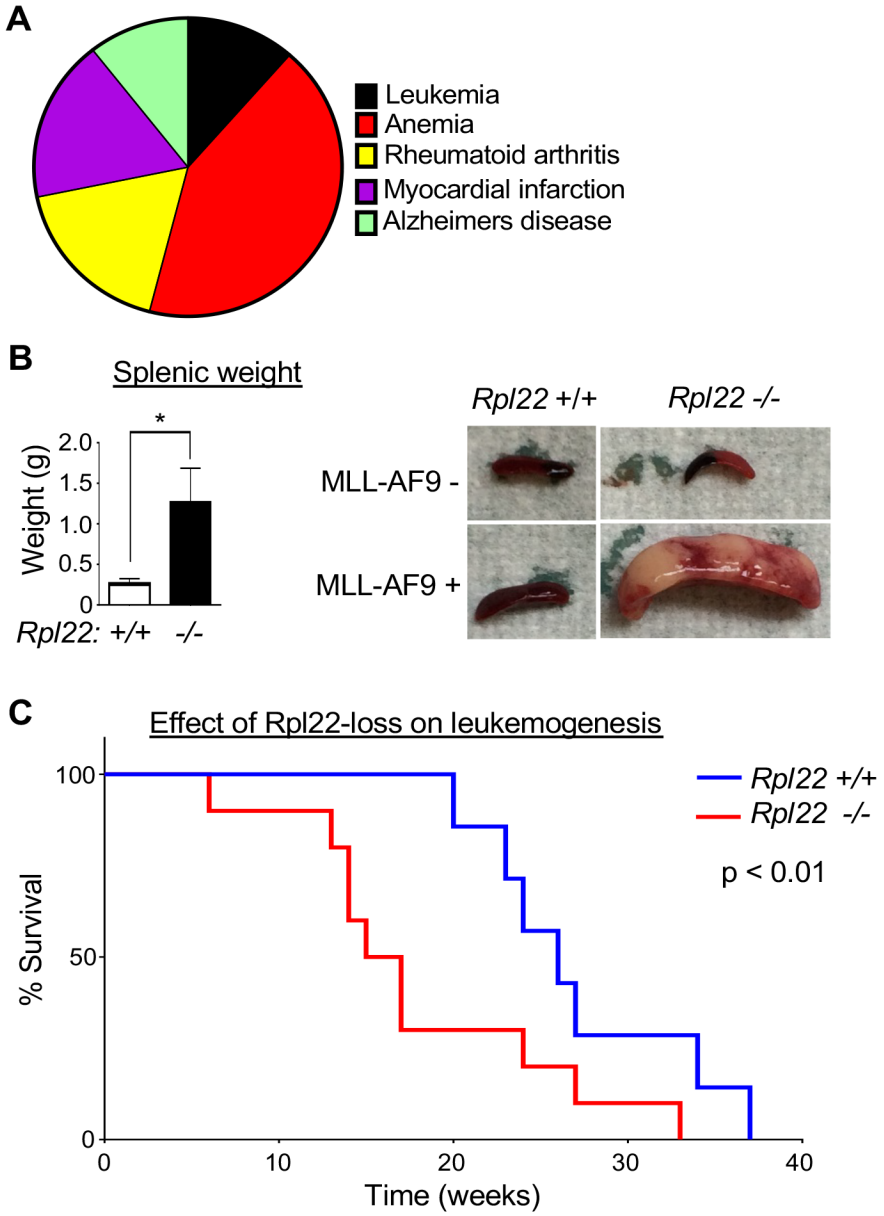

Fig. 6: Rpl22 deficiency facilitates leukemogenesis. (A) OMIM analysis of genes differentially expressed in *Rpl22*-/- HSC. The five most enriched gene sets are depicted graphically as a pie chart. The wedge sizes represent the combined score calculated by EnrichR compared to other categories shown. **(B)** Disease burden on *MLL-AF9* knock in *Rpl22*-/- and *Rpl22*+/+ mice was measured at 15 weeks of age (n = 5). Representative spleens are depicted along with a graphical representation of the mean +/- SEM of splenic weights. ($p < 0.05$) **(C)** Survival analysis of *MLL-AF9* knock in *Rpl22*-/- (n = 10) and *Rpl22*+/+ (n = 7) mice. Significance was determined using a Mantel-Cox test.

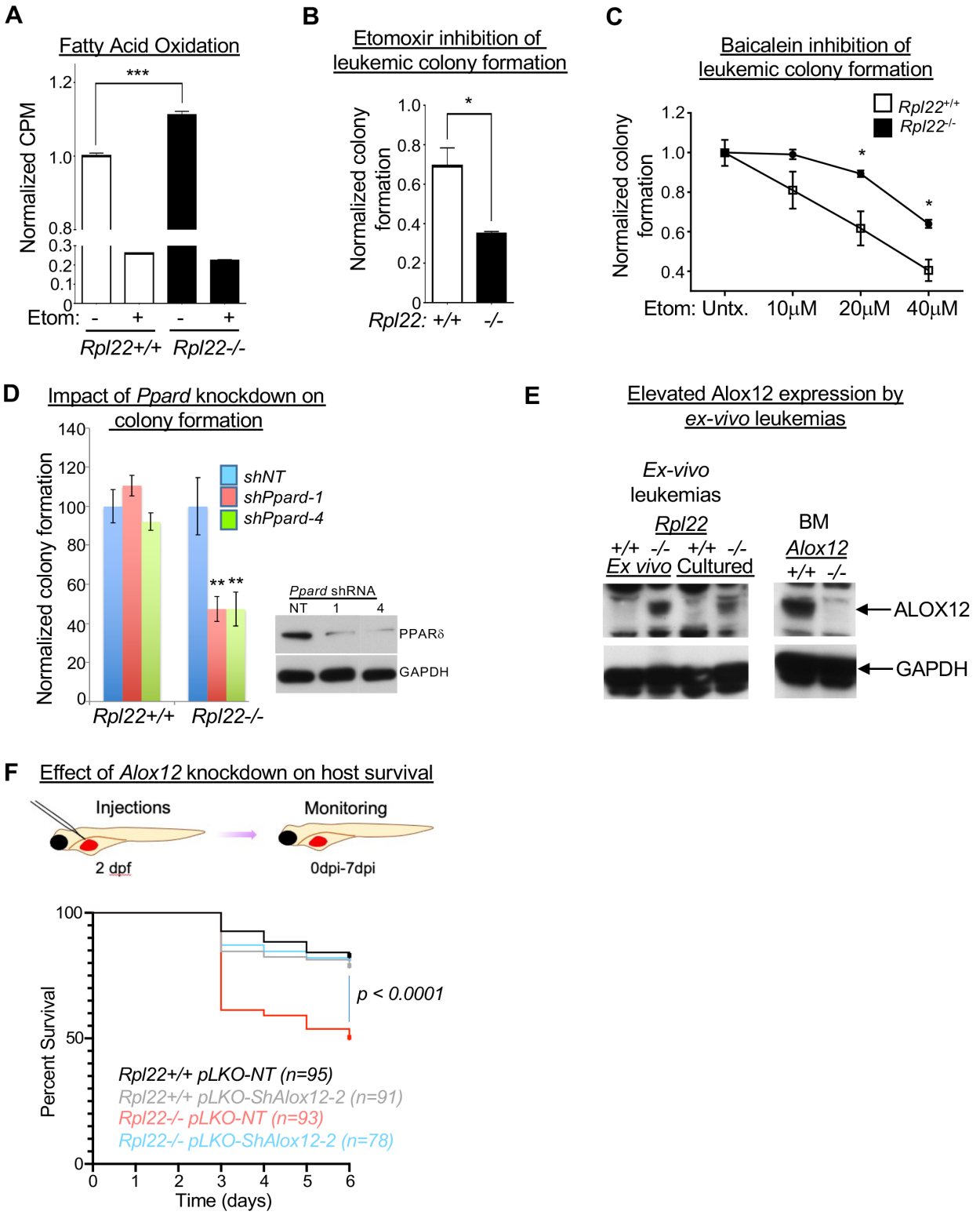

Fig. 7: Rpl22-deficient leukemia cells are sensitive to the loss of ALOX12. (A) Measurement of FAO in MLL-AF9 transformed LSK from *Rpl22*-/- and *Rpl22*+/+ mice. Triplicate measurements of FAO activity are depicted graphically as the mean +/- SEM. **(B)** Effect of Etomoxir treatment

on colony formation by MLL-AF9 transformed LSK cells from *Rpl22*-/- and *Rpl22*+/+ mice. Triplicate measurements of colony formation in methylcellulose are depicted graphically as the mean +/- SEM. **(C)** Graphical representation of the effect of the Alox12 inhibitor, baicalein, on colony formation by MLL-AF9 transduced *Rpl22*+/+ and *Rpl22*-/- LSK. Colony formation was assessed one week after plating (n= 3). Triplicate measurements were graphed as mean +/- SEM and normalized to vehicle treated control. **(D)** PPARδ loss selectively attenuates colony formation by *Rpl22-/-* leukemias. MLL-AF9 transformed leukemias from *Rpl22+/+* and *Rpl22-/-* mice were transduced with shRNA targeting *Ppard* following which their colony forming capacity in methylcellulose was assessed. The mean +/- SEM of triplicate measurements is depicted graphically and the effect of the shRNA on PPARδ expression was assessed on B16 melanoma cells by immunoblotting. **(E)** Leukemia explants from MLL-AF9 knockin *Rpl22+/+* (M82) and *Rpl22-/-* (M109) blotted for Alox12 immediately after isolation (*Ex-vivo)* or after culture in media containing IL3, IL6, and SCF. GAPDH served as a loading control and *Alox12-/-* bonemarrow served as a specificity control. **(F)** Effect of shRNA knockdown of *Alox12* on disease propagation by *Rpl22+/+* and *Rpl22-/-* leukemia cells. Leukemias were lentivirally transduced with either nontargeting (NT) or *Alox12* shRNA (shRNA-2) validated by immunoblotting **(Fig. S7E),** following which the cells were adoptively transferred to zebrafish larvae at 2 days post fertilization (dpf). Survival was monitored for 6 days and depicted graphically. Significance was assessed using Log-rank Matel-Cox testing. All data are representative of 3 separate experiments performed, unless otherwise stated. Unless stated otherwise, all graphs were analyzed for significance using the student's t-test. $^{*}p \leq 0.05$, $^{**}p \leq 0.01$, $^{***}p \leq 0.001$